Direct conversion of adult human skin fibroblasts into functional Schwann cells that achieve robust recovery of the severed peripheral nerve in rats

doi: 10.1002/glia.23582

SPi	Journal Code	Article ID	Dispatch: 19-DEC-18	CE:
	GLIA	23582	No. of Pages: 17	ME:

Received: 9 June 2016 | Revised: 3 December 2018 | Accepted: 11 December 2018

DOI: 10.1002/glia.23582

GLIA

WILEY

RESEARCH ARTICLE

Direct conversion of adult human skin fibroblasts into functional Schwann cells that achieve robust recovery of the severed peripheral nerve in rats

Masaaki Kitada | Toru Murakami | Shohei Wakao | Gen Li | Mari Dezawa

Department of Stem Cell Biology and Histology, Tohoku University Graduate School of Medicine, Sendai, Japan

Correspondence

Mari Dezawa, Department of Stem Cell Biology and Histology, Tohoku University Graduate School of Medicine, 2-1 Seiryo-machi, Aoba-ku, Sendai 980-8575 Japan.
Email: mdezawa@med.tohoku.ac.jp;
and
Masaaki Kitada, Department of Stem Cell Biology and Histology, Tohoku University Graduate School of Medicine, 2-1 Seiryo-machi, Aoba-ku, Sendai 980-8575 Japan.
Email: masaaki.kitada@gmail.com
and
Toru Murakami, Department of Stem Cell Biology and Histology, Tohoku University Graduate School of Medicine, 2-1 Seiryo-machi, Aoba-ku, Sendai 980-8575 Japan.
Email: drtoru56@med.tohoku.ac.jp

Funding information

Japan Society for the Promotion of Science; Ministry of Health, Labor, and Welfare, Japan

Abstract

Direct conversion is considered a promising approach to obtain tissue-specific cells for cell therapies; however, this strategy depends on exogenous gene expression that may cause undesired adverse effects such as tumorigenesis. By optimizing the Schwann cell induction system, which was originally developed for trans-differentiation of bone marrow mesenchymal stem cells into Schwann cells, we established a system to directly convert adult human skin fibroblasts into cells comparable to authentic human Schwann cells without gene introduction. Serial treatments with beta-mercaptoethanol, retinoic acid, and finally a cocktail of basic fibroblast growth factor, forskolin, platelet-derived growth factor-AA, and heregulin-β1 (EGF domain) converted fibroblasts into cells expressing authentic Schwann cell markers at an efficiency of approximately 75%. Genome-wide gene expression analysis suggested the conversion of fibroblasts into the Schwann cell-lineage. Transplantation of induced Schwann cells into severed peripheral nerve of rats facilitated axonal regeneration and robust functional recovery in sciatic function index comparable to those of authentic human Schwann cells. The contributions of induced Schwann cells to myelination of regenerated axons and re-formation of neuromuscular junctions were also demonstrated. Our data clearly demonstrated that cells comparable to functional Schwann cells feasible for the treatment of neural disease can be induced from adult human skin fibroblasts without gene introduction. This direct conversion system will be beneficial for clinical applications to peripheral and central nervous system injuries and demyelinating diseases.

KEYWORDS

axonal regeneration, myelination, PNS injury, re-formation of neuromuscular junction

1 | INTRODUCTION

Recent efforts to direct conversion of somatic cells into other cell types have shown that tissue-specific cells such as neurons (Vierbuchen et al., 2010), oligodendrocyte precursor cells (Najm et al., 2013; Zhu et al., 2014), and other neural-lineage cells (Kim et al., 2014; Ring et al., 2012; Thoma et al., 2014) can be produced by gene transfer of specific transcription factors. A most recent study has even demonstrated that the combination of transcription factors required for direct conversion into any type of cells can be theoretically predicted (Rackham et al., 2016). These induced cells are expected to be hopeful sources for cell therapies; however, most strategies for direct conversion are based on the expression of transgenes that are integrated into the genome of target cells. This genetic modification often interferes with normal gene expression and may cause adverse effects such as tumorigenesis or leukemia formation after transplantation (Hacein-Bey-Abina, Von Kalle, Schmidt, Le Deist, 2003; Hacein-Bey-Abina, Von Kalle, Schmidt, McCormack, 2003). Therefore, direct conversion without gene transfer has the potential to be a safer, more feasible approach to cell therapies.

Schwann cells are glial cells that myelinate axons to allow saltatory conduction in the peripheral nervous system (PNS) (Garbay, Heape, Sargueil, & Cassagne, 2000). They play critical roles in functional repair after PNS damage by stimulating cell proliferation,

Masaaki Kitada and Toru Murakami contributed equally to this study.

producing growth factors and extracellular matrices, constructing Büngner bands that serve as scaffolds for regenerating axons to reach their target, myelinating regenerated axons, and helping synaptic connections at neuromuscular junctions (NMJs) (Allodi, Udina, & Navarro, 2012). Furthermore, Schwann cells retain these functions after transplantation into animal models of central nervous system (CNS) injuries such as those of the optic nerve and spinal cord (Aguayo, David, & Bray, 1981; Dezawa, Kawana, & Adachi-Usami, 1997; Martin et al., 1996) and demyelinating diseases such as multiple sclerosis (Baron-Van Evercooren, Avellana-Adalid, Lachapelle, & Liblau, 1997; Lavdas, Papastefanaki, Thomaidou, & Matsas, 2008; Zujovic et al., 2012). Thus, Schwann cells are expected to be useful in cell therapies applied to both the PNS and CNS. However, several issues have halted clinical application of Schwann cells: a healthy peripheral nerve needs to be sacrificed to harvest Schwann cells; and the technical difficulties of obtaining sufficient human Schwann cells for cell therapy through culture because of their low rate of proliferation. Therefore, a system to induce cells with functions corresponding to those of authentic Schwann cells from other, more easily accessible and highly proliferative cell types would be valuable for clinical applications.

We demonstrated for the first time that bone marrow mesenchymal stem cells (MSCs), which have the high potential to differentiate into ectodermal and endodermal cells as well as mesodermal cells (reviewed in Kitada & Dezawa, 2009; Kuroda, Kitada, Wakao, & Dezawa, 2011), can trans-differentiate into Schwann cells under a specific induction system (Dezawa, Takahashi, Esaki, Takano, & Sawada, 2001). The system includes serial administration of a reducing agent, retinoic acid, and a trophic factor cocktail. Gene transfer is not needed for the induction of Schwann cells. Only 9–10 days are needed to obtain Schwann cells; therefore, the system is highly efficient, with more than 95% of MSCs trans-differentiating into cells functionally equivalent to Schwann cells (Dezawa et al., 2001). In addition, this system was successfully applied to other mesenchymal sources, including bone marrow, adipose tissue, and umbilical cord (Kingham et al., 2007; Peng et al., 2011; Tohill, Mantovani, Wiberg, & Terenghi, 2004) from various animal species, including rats, rabbits, monkeys, and humans (Lu et al., 2008; Wakao et al., 2010; Wang, Luo, Li, & Hu, 2011; Xu et al., 2008). Furthermore, transplantation of Schwann cells induced from macaque monkey bone marrow MSCs showed the long-term safety of this induction system and suggested the feasibility of its use (Wakao et al., 2011). Therefore, clinical application of this Schwann cell induction system is expected to be valuable for the treatment of PNS and CNS injury and demyelinating diseases.

In this study, we asked the possibility to apply adult human skin fibroblasts, whose origin is the same as that of MSCs but that are considered highly differentiated cells, to this induction system for direct conversion into functional Schwann cells. Because fibroblasts are easily accessible and can be expanded to clinical scale with reasonable time and cost, successful conversion of fibroblasts into functional Schwann cells would be of great interest. We examined the properties of adult human skin fibroblasts treated with the Schwann cell induction system in vitro and validated their neuro-regenerative functions in vivo by grafting these cells into a rat PNS injury model.

2 | MATERIALS AND METHODS

2.1 | Cultures

Adult human skin fibroblasts were purchased from Lonza (normal human dermal fibroblasts-adult, Basel, Switzerland). They were maintained in α-modification Eagle's minimal essential medium (α-MEM; M4526, Sigma-Aldrich, St. Louis, MO, USA) with 10% fetal bovine serum (FBS; Hyclone, GE Healthcare Life Sciences, South Logan, UT, USA) and 0.1 mg/mL kanamycin (Gibco, Thermo Fisher Scientific, Waltham, MA, USA).

Human Schwann cells (described hereafter as "primary human Schwann cells" [ScienCell, Carlsbad, CA, USA]), were maintained in Schwann cell medium (ScienCell).

2.2 | Direct conversion of fibroblasts into Schwann cells

Fibroblasts were treated with the Schwann cell induction system, which was originally developed by Dezawa et al. for the trans-differentiation of bone marrow MSCs into Schwann cells (Dezawa et al., 2001). We optimized this system to directly convert adult human skin fibroblasts into Schwann cells (hereafter described as "induced Schwann cells"). A schematic illustration of this induction system with optimization is shown in Figure 1. Adult human skin fibroblasts from passage 5 to 9 were plated at a density of 790 cells/cm^2 with 10% FBS in α-MEM. On the next day, the medium was changed to α-MEM containing 1 mM β-mercaptoethanol (BME) without serum, and the cells were incubated for another 24 hr. The medium was then replaced with α-MEM containing 10% FBS and 35 ng/mL all-trans retinoic acid (RA; Sigma-Aldrich). Three days later, the cells were washed with phosphate-buffered saline (PBS) and cultured in a medium comprising α-MEM, 10 ng/mL recombinant human basic fibroblast growth factor (bFGF; Wako, Osaka, Japan), 5 μM forskolin (Millipore, Darmstadt, Germany), 10 ng/mL platelet-derived growth factor-AA (PDGF-AA; Peprotech, Rocky Hill, CT, USA), and 200 ng/mL heregulin-β1-EGF domain (HRG; R&D Systems, Minneapolis, MN, USA) for 4 days. To optimize this induction system, medium with 10, 5, or 1% FBS was used during the treatment with the cocktail of trophic factors, and the effects of the different FBS concentrations were compared (Figure 1).

2.3 | Flow cytometry and fluorescence-activated cells sorting (FACS)

For analyzing the cell surface antigen expression, cultured cells were harvested and incubated with one of the following primary antibodies: Phycoerythrin (PE) conjugated-anti-CD44 mouse IgG (1:40; Beckton Dickinson, Frankin Lakes, NJ, USA), PE-anti-CD73 mouse IgG (1:40; Beckton Dickinson), PE-anti-CD90 mouse IgG (1:40; Beckton Dickinson), PE-anti-CD34 mouse IgG (1:40; Beckton Dickinson), PE-anti-CD45 mouse IgG (1:40; Beckton Dickinson), PE-anti-CD271 (1:50; Beckton Dickinson) mouse IgG, PE-anti-CD117 mouse IgG (1:50; Beckton Dickinson), and anti-Stage-specific embryonic antigen-3 (SSEA-3) rat IgM (1:100; Millipore). The secondary antibody for the

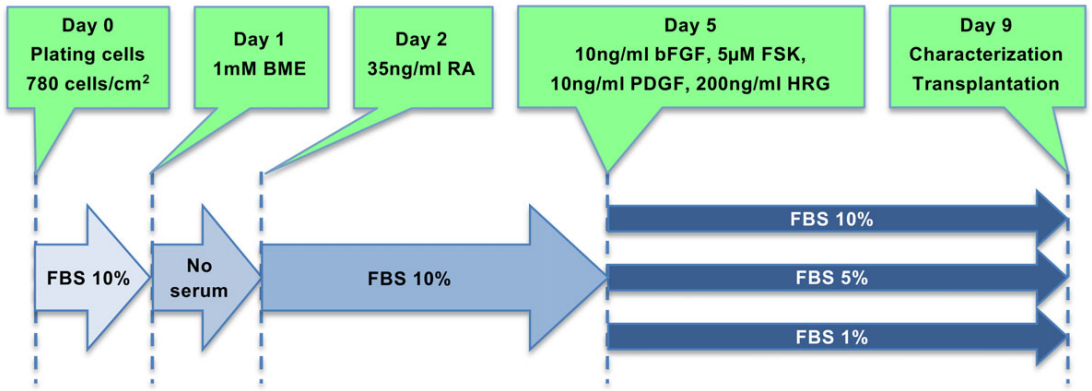

FIGURE 1 A schematic illustration of the Schwann cell induction system with optimization of the serum concentration for direct conversion of adult human skin fibroblasts into Schwann cells. FBS, fetal bovine serum; BME, β-mercaptoethanol; RA, all-trans retinoic acid; FSK, forskolin; bFGF, basic fibroblast growth factor; PDGF, platelet-derived growth factor-AA; HRG, heregulin-β1-EGF domain

detection of anti-SSEA-3 rat IgM was Allophycocyanin-conjugated anti-rat IgM goat IgG (1:100; Jackson Immunoresearch, West Grove, PA, USA). For cell sorting of the cell population triple-negative for CD271, CD117, and SSEA-3, cells were harvested and incubated with three antibodies mentioned above followed by the incubation of the secondary antibody against rat IgM. Flow cytometry and FACS were performed with FACSAria II Special Order Products (Beckton Dickinson). The negative controls of flow cytometry and FACS were taken with or without the corresponding isotype controls and the secondary antibody.

2.4 | Immunocytochemistry

Cultured cells were fixed with 4% paraformaldehyde (PFA) in 0.1 M phosphate buffer (PB) and subjected to immunocytochemistry as described previously (Kuroda et al., 2013). After blocking, cells were incubated with one of the following primary antibodies: anti-p75 nerve growth factor (NGF) receptor (p75) mouse IgG (1:500; Abcam, Cambridge, England), anti-protein zero (P0) mouse IgG (1:100; kindly provided by Dr. J. J. Archelos, Karl-Franzens Universitat, Graz, Austria), anti-GFAP rabbit IgG (1:300; DAKO, Glostrup, Denmark), anti-S100 rabbit IgG (1:800; DAKO), anti-O4 mouse IgM (1:50; Millipore), anti-Sox10 rabbit IgG (1:500; Abcam), anti-POU3F1 mouse IgG (1:300; Santa Cruz, Dallas, TX, USA), and anti-Krox20 mouse IgG (1:100; OriGene, Rockville, MD, USA). The secondary antibodies used for immunocytochemistry were labeled with Alexa Fluor 488 or 568: anti-mouse Ig donkey IgG and anti-rabbit Ig donkey IgG (1:500; Thermo Fisher Scientific, Carlsbad, CA, USA). Nuclei were counterstained with 4′,6-diamidino-2-phenylindole (DAPI, Sigma-Aldrich).

2.5 | Reverse-transcription polymerase chain reaction (RT-PCR)

mRNAs were purified using an RNeasy Mini Kit (Qiagen, Venlo, Netherlands), and then complementary DNA (cDNA) was reverse-transcribed with SuperScript III Reverse Transcriptase (Thermo Fisher Scientific) following the manufacturer's protocol.

The following primers were used for the amplification of specific gene products:

P0 (373 bp) forward 5′-CAGAGGAGGCTCAGTGCTATGG-3′, reverse 5′-GCGATCACTTGTCCGAGTTCAG-3′; S100B (405 bp) forward 5′-CGAACTGAAGGAGCTCATCAAC-3′, reverse 5′-GCTTACAC ACAGGCCTAATATAGC-3′; SOX10 (325 bp) forward 5′-CCACCCGG ACTACAAGTACC-3′, reverse 5′-GTTGCCGAAGTCGATGTGAG-3′; KROX20 (483 bp) forward 5′-CACCAGCTGTCTGACAACATCTAC-3′, reverse 5′-CCTGCACAGCCAGAATAAGG-3′; β-actin (220 bp) forward 5′-AGGCGGACTATGACTTAGTTGCGTTACACC-3′, reverse 5′-AAG TCCTCGGCCACATTGTGAACTTTG-3′. Primary human Schwann cells were used as positive controls.

2.6 | Quantitative reverse-transcription polymerase chain reaction (qRT-PCR)

For qRT-PCR, cDNA was obtained by reverse transcription from mRNA using a SuperScript VILO cDNA Synthesis Kit (Thermo Fisher Scientific) and then amplified with primer mixes from Taqman Gene Expression Assays (Thermo Fisher Scientific) for ERBB3, ITGA4, TFAP2A, GFAP, and POU3F1 using a 7,500 Fast Real-Time PCR System (Applied Biosystems, Thermo Fisher Scientific) according to the manufacturer's instructions. Data were obtained using the ΔΔCt method (Livak & Schmittgen, 2001) and normalized by mRNA levels in primary human Schwann cells.

2.7 | RNA-seq

RNA-seq was conducted for the comparison of the genome-wide gene expression profile. Because a certain fraction of fibroblasts is contaminated in the culture of both induced Schwann cells and primary human Schwann cells, we eliminated cells positive for CD90, one of the typical mesenchymal cell markers, from induced Schwan cells and primary human Schwann cells by FACS and then remaining cells were subjected to RNA-seq. Anti-CD90 mouse IgG conjugated to allophycocyanin (1:100; Becton Dickinson) was used for cell sorting. On the other hand, a CD90-positive population was collected from adult human skin fibroblasts. Total mRNA was extracted from the three samples, CD90(−)-induced Schwann cell fraction, CD90 (−)-primary human Schwann cell fraction and CD90(+) human fibroblasts by Nucleospin RNA XS (Macherey-Nagel Gmbh, Düren,

Germany). The poly(A) RNA selection was performed with NEBNext Poly(A) mRNA Magnetic Isolation Module (New England Biolabs, Ipswitch, MA, USA), and the libraries for RNA sequencing were constructed using NEBNext Ultra II RNA Library Prep Kit for Illumina (New England Biolabs). The fragmented and randomly primed 150-bp paired-end libraries were sequenced using Illumina Hiseq 2,500 (Illumina, San Diego, CA, USA). The mapping of the sequenced data was performed using the HISAT2 program. The heatmap with clustering analysis were conducted with the gplots program. Normalized differentially expressed genes were detected by the DESeq2 program, where a twofold-change threshold cutoff was set for the detection of significantly up- or down-regulated genes. Gene set enrichment analysis was conducted with the DAVID program (http://david.abcc.ncifcrf.gov/). The qualification and poly(A) selection of mRNA, library construction, sequencing, and analysis of RNA-seq data were outsourced to GENEWIZ (South Plainfield, NJ, USA).

2.8 | Cell preparation for transplantation

All animal experiments were approved by the Ethics Committee for Animal Experiments at Tohoku University, and all gene recombination experiments were approved by the Committee for Gene Experiments at Tohoku University. Male Wistar rats (8 weeks old) were used for transplantation experiments. Prior to transplantation, fibroblasts, induced Schwann cells, and primary human Schwann cells were infected with the lentivirus encoding green fluorescent protein (GFP) under the ubiquitous promoter of human EF1-alpha as previously described (Nguyen, Khakhoulina, Simmons, Morel, & Trono, 2005; Shimizu et al., 2007) to distinguish transplanted cells from endogenous recipient Schwann cells. Cells were collected, suspended in Matrigel (BD Bioscience, Becton Dickinson) at a concentration of 1.0×10^5 cells/μl, and transferred into 6-mm long transpermeable tubes (Millipore) to prepare artificial grafts as previously described (Matsuse et al., 2010; Shimizu et al., 2007). In total, 1.0×10^5 cells were added to each graft, except for the Matrigel-only group.

2.9 | Transplantation to the severed peripheral nerve in rats

Complete transection of the peripheral nerve in rats and transplantation of the artificial graft containing the cultured cells were performed as previously described (Matsuse et al., 2010; Shimizu et al., 2007). Briefly, a segment of the sciatic nerve in each animal was removed from the middle of the left thighbone under general anesthesia with isoflurane to create a 5-mm gap. Transplantation was performed by connecting the gap with the artificial graft containing the cells using 10-0 nylon sutures. For the negative control, animals were transplanted with tubes containing only Matrigel. Six animals were used per group for the fibroblast and induced Schwann cell groups, seven animals were used for the primary human Schwann cell group, and five animals were used for the Matrigel-only group. After transplantation of the artificial grafts, 0.5 mg/kg FK506 (Astellas Pharma, Inc., Tokyo, Japan) was administrated subcutaneously each day for immunosuppression. We made an autograft model as another control: a complete transection of the sciatic nerve to make a 6-mm gap as described above, and tied the removed segment to the sciatic nerve again by suturing. Four animals were used for the autograft group.

2.10 | Immunohistochemistry

Six weeks after transplantation, transcardial perfusion with periodate-lysine-paraformaldehyde fixatives was performed under an overdose of anesthesia, and the sciatic nerve, including the artificial graft and the flexor digitorum brevis muscle, was dissected from the affected side of the rat. The tissues were fixed using the same fixatives at 4 °C overnight. These fixatives were successively displaced by 15, 20, and 25% sucrose in 0.02 M PBS. The tissues were embedded in OCT compound, frozen on dry ice, and sliced into 10-μm sections.

After blocking, the tissues were incubated with one of the following primary antibodies overnight at 4 °C, and then incubated with the corresponding secondary antibody. Primary antibodies used were: anti-neurofilament rabbit IgG (1:200; Millipore), anti-myelin basic protein (MBP) mouse IgG (1:300; Millipore), anti-GFP rabbit IgG (1:100; Abcam), anti-GFP chicken IgY (1:1000; Abcam), and anti-synaptophysin mouse IgG (1:1000; Millipore). Secondary antibodies: anti-rabbit Ig donkey IgG conjugated with Alexa Fluor 488 or 568, anti-mouse Ig donkey IgG conjugated with Alexa Fluor 568 or 680 (1:500; Thermo Fisher Scientific), and anti-chicken Ig goat IgG conjugated with Alexa Fluor 488 (1:500; Thermo Fisher Scientific). Nuclei were counterstained with DAPI, and samples were inspected under a laser confocal microscope system (C2 Nikon Confocal Microscope System).

To assess the number of axons in each portion of the graft, transverse sections from three animals in each transplanted group were made. The sections were cut at 2-, 4-, and 6-mm from the proximal end of the graft. After immunostaining for neurofilament and MBP in the transverse sections at the 6-mm position from the proximal end of the graft, the numbers of axons and myelinated axons observed was counted using Image J (National Institutes of Health, Bethesda, MD, USA). In the transverse section of the graft, we determined "the outer area" of the graft as the area near by the wall of the graft tube, whose distance from the tube was up to 300 μm. Also, "the inner area" in the transverse section of the graft was determined as the circular area containing the center of the graft, whose diameter was up to 300 μm.

To estimate the reformation of NMJs, sections parallel to the flexor digitorum brevis muscle were cut and subjected to double staining for synaptophysin and with FITC-labeled α-bungarotoxin (1:100; Thermo Fisher Scientific). NMJs in each section were manually counted in six sections per animal from at least three animals. The number of NMJs in the uninjured animals was also evaluated.

2.11 | Conventional electron microscopy

Six weeks after transplantation, animals of the fibroblast group was transcardial perfused with 2.5% glutaraldehyde and 2.0% paraformaldehyde in 0.1 M PBS under an overdose of anesthesia, and the sciatic nerve including the artificial graft was dissected from the affected side of the rat. The tissues were further fixed using the same fixatives at 4 °C overnight, washed in 0.1 M PBS, and post-fixed with 1.0% osmium tetroxide in 0.1 M PBS. The samples were dehydrated with the sequential concentration of ethanol and

propylene oxide, substituted to epoxy resin, cut into ultrathin section, and observed under electron microscope (JEM-1011, JEOL, Akishima, Tokyo, Japan).

2.12 | Immunoelectron microscopy

Immunoelectron microscopy was performed as previously described (Kitada, Chakrabortty, Matsumoto, Taketomi, & Ide, 2001). Briefly, the rats were deeply anesthetized by inhalation of isoflurane and perfused through the heart with 4% PFA/0.1 M PBS 6 weeks after transplantation of the artificial nerve graft containing induced Schwann cells. The sciatic nerve was excised, post-fixed with the same fixatives, and treated with the same procedure described in the "Immunocytochemistry" section. Sections were incubated with 20% Block Ace (DS Pharma Biomedical, Osaka, Japan), 5% bovine serum albumin (BSA, Nacalai Tesque), 0.01% saponin, and 0.02 M PBS for 1 hr, followed by incubation with anti-GFP rabbit IgG (Abcam) in 5% Block Ace, 1% BSA, 0.01% saponin, and 0.02 M PBS two overnights at 4 °C. Sections were then incubated with anti-rabbit IgG goat IgG conjugated to 1.4 nm Nanogold (Nanoprobes Inc., Stony Brook, NY) two overnights at 4 °C. The signal of Nanogold was enhanced using HQ Silver (Nanoprobes) for visualization by electron microscopy.

2.13 | Behavioral analysis

A walking track analysis was performed every week for 6 weeks after transplantation as previously described (Bain, Mackinnon, & Hunter, 1989; Matsuse et al., 2010; Shimizu et al., 2007; Varejao, Meek, Ferreira, Patricio, & Cabrita, 2001). The hind feet of the rats were painted uniformly with black finger paint. The animal was allowed to walk on the paper in a tunnel, leaving its footprints. We measured the distance between (1) heel and toe (PL), (2) the first and fifth toe (TS), and (3) the second and fourth toe, and then calculated the sciatic function index (SFI) according to the following formula (e = experimental side, n = normal side):

$$SFI = -38.3 \times \frac{PL_e - PL_n}{PL_n} + 109.5 \times \frac{TS_e - TS_n}{TS_n} + 13.3 \times \frac{ITS_e - ITS_n}{ITS_n} - 8.8$$

2.14 | Statistical analysis

Numerical data, including the rate of cells positive for Schwann cell markers in immunocytochemistry, the number of axons and the rate of myelination of regenerated axons in a transverse section, the SFI score, and the number of NMJs, are expressed as mean ± standard error. Welch's *t* test with the Bonferroni correction for multiple comparisons was used for comparisons between groups. A paired *t*-test with the Bonferroni correction was used for comparisons within groups. The number of animals used for statistical analysis of the numbers of neurofilament-positive axons and NMJs and the rate of myelination of regenerated axons were 3 and 4 in each group, respectively. The SFI scores were 6, 7, 6, 3, and 3 for the induced Schwann cell, primary human Schwann cell, fibroblast, Matrigel-only, and autograft groups, respectively.

3 | RESULTS

3.1 | Optimization of the induction system for direct conversion of human fibroblasts into Schwann cells

In previous reports of Schwann cell induction from bone marrow and umbilical cord MSCs, 10% FBS was used for culture (Dezawa et al., 2001; Matsuse et al., 2010; Shimizu et al., 2007). However, adult human skin fibroblasts proliferate faster than MSCs when they are cultured in 10% FBS, and they become over-confluent in the early phase of the final induction step. Hence, they fail to convert into Schwann cells. Therefore, we tested three FBS concentrations, 10, 5, and 1%, in the final induction step to compare induction efficiency.

Naïve fibroblasts have large, flattened cytoplasm. Following sequential treatments with BME, RA, and trophic factors, some of fibroblasts gradually changed their morphology to a small, spindle-shaped, which was similar to that of authentic primary human Schwann cells (Figure 2a). We then measured the percent of cells that were positive for p75, a marker for neural crest cells, Schwann cell precursors, and mature Schwann cells (Jessen & Mirsky, 2005). The percentages of p75-positive cells in 10, 5, and 1% FBS were 48.8 ± 1.4%, 74.6 ± 0.6%, and 50.8 ± 4.7%, respectively, indicating that the highest proportion was found in 5% FBS (Figure 2b). In addition, Schwann cell marker S100B (Jessen et al., 1994) was only detected by RT-PCR in 5% FBS (Figure 2c). Based on these results, we eventually selected 5% FBS as the best serum concentration during the final step of the induction of Schwann cells from adult human skin fibroblasts.

3.2 | Assessment of fibroblast-derived Schwann cells

The expression of authentic Schwann cell markers in induced Schwann cells was analyzed. Immunocytochemistry was performed with antibodies against p75, P0 (a marker for Schwann cell precursors and immature and mature Schwann cells [Lee et al., 1997]), GFAP (a marker for immature and nonmyelinating Schwann cells [Jessen, Morgan, Stewart, & Mirsky, 1990; Mirsky et al., 2008]), S100, and O4 (a marker for immature and mature Schwann cells [Dong et al., 1999]). Although none of these markers were detected in naïve fibroblasts, the percentage of induced Schwann cells that were positive for P0, GFAP, S100, and O4 were 22.8 ± 5.8%, 51.9 ± 3.1%, 56.4 ± 8.0%, and 16.9 ± 1.2%, respectively. The percentage of fibroblasts that were p75 positive was 74.6 ± 0.6%, as shown above. Authentic primary human Schwann cells were also positive for p75, P0, GFAP, S100, and O4, with percentages of cells that were positive of 60.2 ± 1.5%, 36.7 ± 4.7%, 41.1 ± 2.3%, 59.3 ± 7.3%, and 32.4 ± 4.4%, respectively (Figure 3a). The expression of other Schwann cell markers such as Sox10, POU3F1, and Krox20 in induced Schwann cells was also confirmed (Supporting Information Figure S1), and double immunostaining for p75/S100, p75/GFAP, and Sox10/POU3F1 demonstrated that the same cells jointly expressed these Schwann cell markers (Supporting Information Figure S2).

We then confirmed the expression of primary human Schwann cell markers in induced Schwann cells by RT-PCR. While none of the mRNAs for Schwann cell markers were detected in fibroblasts, induced

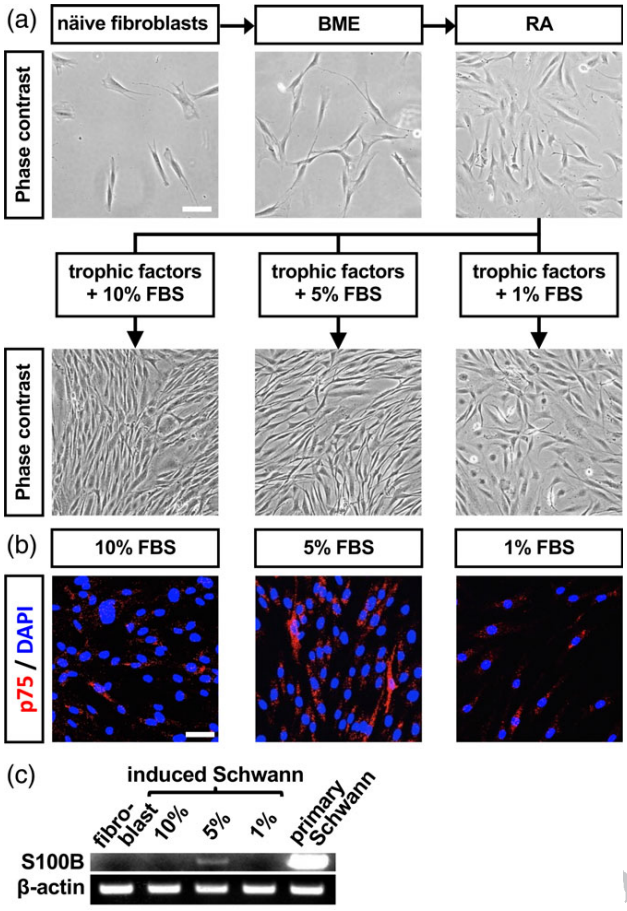

Color Figure ? Print and Online

FIGURE 2 Optimization of the Schwann cell induction system for adult human skin fibroblasts. (a) Morphological changes in fibroblasts before (näive fibroblast) and after sequential treatments with β-mercaptoethanol (BME), all-trans retinoic acid (RA), and trophic factors in 10, 5, or 1% fetal bovine serum (FBS)-containing medium. (b) Immunocytochemistry against p75, a marker for Schwann cell precursors and mature Schwann cells. After Schwann cell induction from fibroblasts with 10, 5, or 1% FBS, cells positive for p75 (red) were induced from fibroblasts. Fibroblast-derived Schwann cells induced with 5% FBS exhibited the highest proportion of p75-positive cells. Nuclei were visualized with DAPI (blue). (c) The expression of S100B mRNA in fibroblasts (fibroblast) and induced Schwann cells (induced Schwann) treated with each FBS concentration. The expression of S100B mRNA was only detected in the 5% FBS treatment. Primary human Schwann cells (primary Schwann) were used as a positive control. Scale bars: (a) 100 μm; (b) 50 μm

Schwann cells expressed P0, S100B, SOX10 (a transcription factor expressed in neural crest cells, Schwann cell precursors, immature Schwann cells, and mature Schwann cells and critical for the specification of neural crest cells into peripheral glia, sequential differentiation of immature Schwann cells into myelinating Schwann cells, and maintenance of myelin) (Finzsch et al., 2010; Schreiner et al., 2007; Stolt & Wegner, 2016; Wegner, 2000; Weider & Wegner, 2017; Woodhoo & Sommer, 2008), and KROX20 (a transcription factor expressed from pre-myelinating to mature Schwann cells and indispensable for myelination and maintenance of myelin) (Monk, Feltri, & Taveggia, 2015; Salzer, 2015; Stolt & Wegner, 2016; Sung et al., 1998; Svaren & Meijer, 2008; Topilko et al., 1994; Wegner, 2000; Woodhoo & Sommer, 2008), similar to primary human Schwann cells (the positive control). Thus, the expression pattern of Schwann cell markers in induced Schwann cells resembled that of authentic Schwann cells (Figure 3b).

Next, we evaluated the expression levels of mRNAs involved in Schwann cell development at each point in Schwann cell induction (Figure 3c). ERBB3, which is expressed consistently throughout Schwann cell development and is critical for the intracellular signaling of proliferation, survival, and migration of Schwann cell precursors and early Schwann cells (Garratt, Britsch, & Birchmeier, 2000; Grigoryan & Birchmeier, 2015; Riethmacher et al., 1997), was substantially upregulated after BME treatment and was maintained in induced Schwann cells. ITGA4 and TFAP2A, both expressed in neural crest cells, Schwann cell precursors, and immature Schwann cells (Haack & Hynes, 2001; Joseph et al., 2004; Mitchell, Timmons, Hebert, Rigby, & Tjian, 1991; Stewart et al., 2001; Sung et al., 1998), were upregulated after either BME or RA treatment. GFAP, expressed in immature and nonmyelinating Schwann cells, increased after treatment with RA, and was highly upregulated in induced Schwann cells. POU3F1, expressed in immature and pre-myelinating Schwann cells and regulating the progression from pre-myelinating to the myelinating phenotype collaborating with POU3F2 (Salzer, 2015; Stolt & Wegner, 2016; Zorick, Syroid, Arroyo, Scherer, & Lemke, 1996), was detected during induction, and the expression levels of this factor in induced Schwann cells were almost the same as those in primary human Schwann cells (Figure 3c).

We further performed genome-wide gene expression profiling to confirm the conversion of adult human skin fibroblasts into the Schwann cell-lineage (Figure 4 and Supporting Information Figure S3). Principal component analysis revealed a clear difference between three cell populations, namely fibroblasts, induced Schwann cells, and primary human Schwann cells (Figure 4a). We focused on the expression of particular gene sets by the heatmap and clustering analysis. Although the expression pattern of some gene sets such as genes associated with cell adhesion and extracellular matrix expressed in induced Schwann cells exhibited more similarity to those expressed in fibroblasts than those in primary human Schwann cells (Figure 4b and Supporting Information Figure S3A), the expression profile of transcription factors and growth factors in induced Schwann cells was more similar to that in primary human Schwann cells (Figure 4c,d). Gene set enrichment analysis of induced Schwann cells compared with adult human skin fibroblasts showed the up-regulation of the gene sets related to the cell signaling of Wnt, bFGF, bone morphogenetic protein (BMP), and transforming growth factor (TGF)-beta (Supporting Information Figure S3B), which are known to be activated in the neural crest-derived cell lineages including Schwann cells and their precursors (Jacob, Grabner, Atanasoski, & Suter, 2008; Stewart et al., 1995; Villanueva, Glavic, Ruiz, & Mayor, 2002). The down-regulation of gene sets with relevance to the development or function of mesenchymal cells such as mesenchymal cell development, extracellular exosome, would healing, and adherens junction was also confirmed (Supporting Information Figure S3B). The gene expression profile further demonstrated that induced Schwann cells presented higher expression of genes associated to cell cycle compared with primary human Schwann cells (Supporting Information Figure S3C). These findings collectively imply that induced Schwann cells gradually lose the characteristics of mesenchymal cells and acquire those of the Schwann cell-lineage.

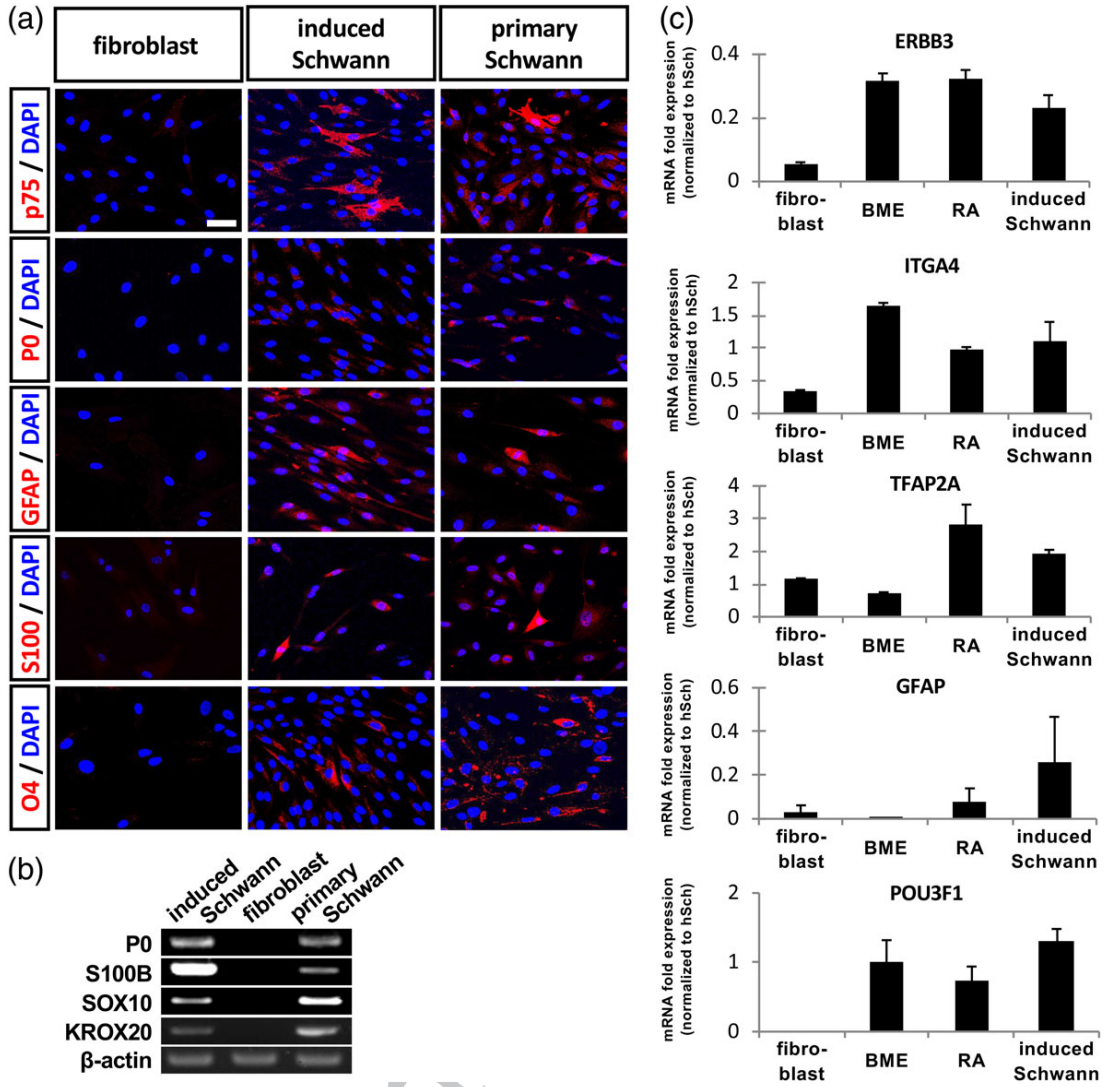

FIGURE 3 The expression of Schwann cell markers in induced Schwann cells. (a) Immunocytochemistry for Schwann cell markers p75, P0, GFAP, S100, and O4, in fibroblasts (fibroblast), induced Schwann cells (induced Schwann), and primary human Schwann cells (primary Schwann). Nuclei were counterstained with DAPI (blue). (b) The mRNA expression of Schwann cell markers P0, S100B, SOX10, and KROX20 in primary human Schwann cells (primary Schwann), fibroblasts (fibroblast), and induced Schwann cells (induced Schwann). (c) Quantitative RT-PCR evaluation of the expression of genes involved in Schwann cell development from fibroblasts before the treatments (fibroblast) and after sequential treatment with β-mercaptoethanol (BME), all-trans retinoic acid (RA), and trophic factors with 5% serum (induced Schwann). The expression level of each gene is indicated by the mRNA fold-expression normalized to that of primary human Schwann cells. Scale bars: (a), 50 μm

3.3 | Transplantation of induced Schwann cells into a transected rat sciatic nerve model

Supporting the regeneration of axons is one of important functions of Schwann cells in nerve regeneration. To evaluate the ability of induced Schwann cells in nerve regeneration, we transplanted an artificial graft composed of a permeable tube filled with Matrigel and either fibroblasts induced Schwann cells, or primary human Schwann cells into the gap of a transected rat sciatic nerve. These cells were labeled with GFP using a lentivirus prior to the transplantation. Six weeks after transplantation, the site of injury was opened and observed. Whereas the parenchymal tissue inside the graft was reddish and appeared vulnerable in the fibroblast group, that of the induced Schwann cell and primary human Schwann cell groups seemed whitish and solid (Figure 5a).

To evaluate axonal regeneration in each experimental group, immunohistochemistry for neurofilament was performed on transverse sections 2, 4, and 6 mm from the proximal end of each graft 6 weeks after transplantation. Compared with the fibroblast group, a larger number of neurofilament-positive signals were detected at each sampling point from the proximal end of the graft of the induced Schwann cell or primary human Schwann cell groups (Figure 5b). To evaluate the extent of axonal regeneration, we counted the number of neurofilament-positive axons in each section. At all three positions, the number of neurofilament-positive axons was greater in the induced Schwann cell group compared with those in the Matrigel-only and fibroblast groups. Notably, the number of neurofilament-positive axons in the induced Schwann cell group at the 6-mm position was significantly greater than those in the Matrigel-only and fibroblast

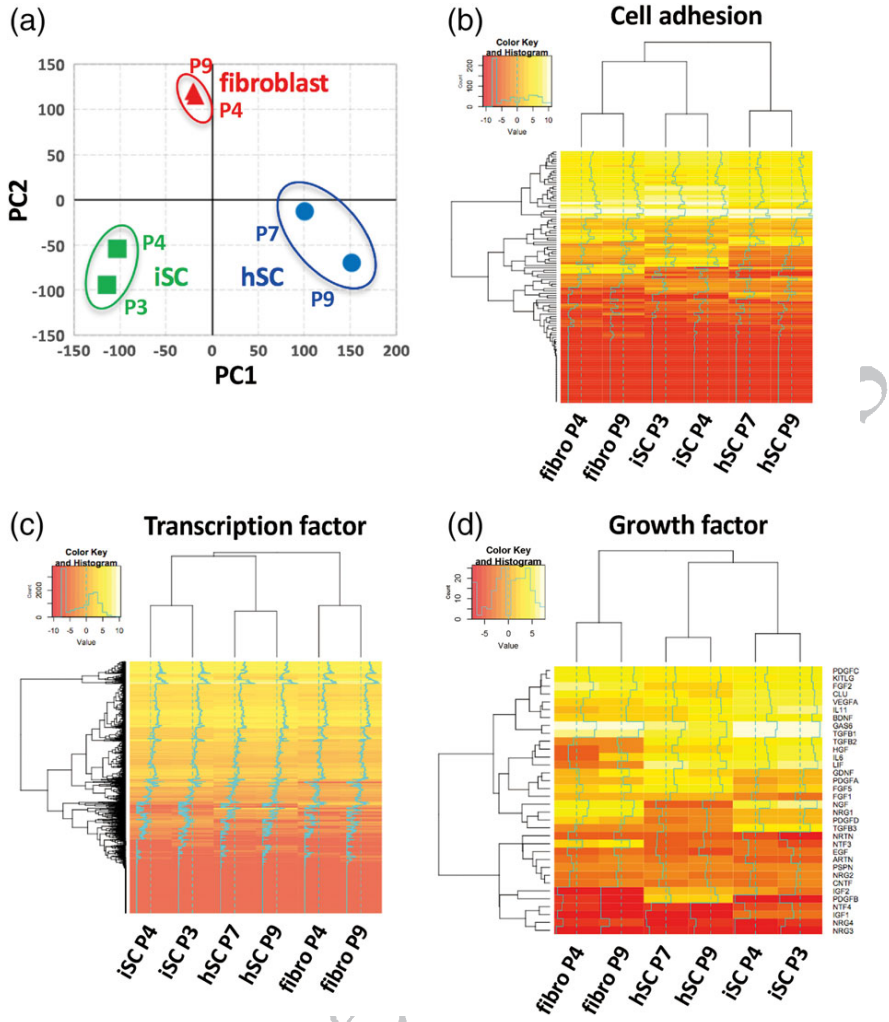

Color Figure - Print and Online

FIGURE 4 Genome-wide gene expression analysis. (a) Principal component analysis of mRNA expression profiles from adult human skin fibroblasts (fibroblast), induced Schwann cells (iSC), and primary human Schwann cells (hSC). Principal components of 1 (x axis) and 2 (y axis) account for 34.4 and 26.8% of the variation of the data sets, respectively. (b–d) The heatmap with clustering of the expression profile of particular gene sets. The heatmaps of the expression of gene sets for cell adhesion (b), transcription factors (c), and growth factors (d) in adult human skin fibroblasts (fibro), induced Schwann cells (iSC), and primary human Schwann cells (hSC) were shown. The number after "P" indicated the passage number of each cell culture

groups (both $p < 0.05$; Figure 5c). In contrast, there was no significant difference in the numbers of neurofilament-positive axons between the induced Schwann cell and primary human Schwann cell groups at any of the three sites. Similarly, there was no statistical difference in the Matrigel-only and fibroblast groups at all three positions. The autograft group showed the greatest numbers of neurofilament-positive axons among all groups at all three positions, but there were no statistical differences in the induced Schwann cell and autograft groups at the 2- and 4-mm positions (Figure 5c). Detailed histological analysis elucidated the difference in the extent of axonal regeneration between the inner and outer areas of the graft (see Materials and methods) at the 6-mm position (Supporting Information Figure S4). As for the outer area of the graft, there was no statistical difference in the numbers of regenerated axons observed in the fibroblast (534.4 ± 16.5 axons/1000 μm^2), induced Schwann cell (533.2 ± 8.16 axons/1000 μm^2), and primary human Schwann cell (508.4 ± 11.4 axons/1000 μm^2) groups. However, that in the inner area of the graft in the induced Schwann cell group (600.4 ± 28.4 axons/1000 μm^2) was significantly higher than that in the fibroblast group (40.4 ± 2.72 axons/1000 μm^2), whereas there was no statistical difference between the induced Schwann cell and primary human Schwann cell (532.0 ± 45.6 axons/1000 μm^2) groups (Supporting Information Figure S4). These findings suggest that transplantation of induced Schwann cells promote axonal regeneration to an extent that is comparable to that of primary human Schwann cells.

3.4 | The myelination ability of induced Schwann cells after transplantation

Myelination of regenerated axons is the other important function of Schwann cells in nerve regeneration. To examine the myelination ability of induced Schwann cells after transplantation, we performed

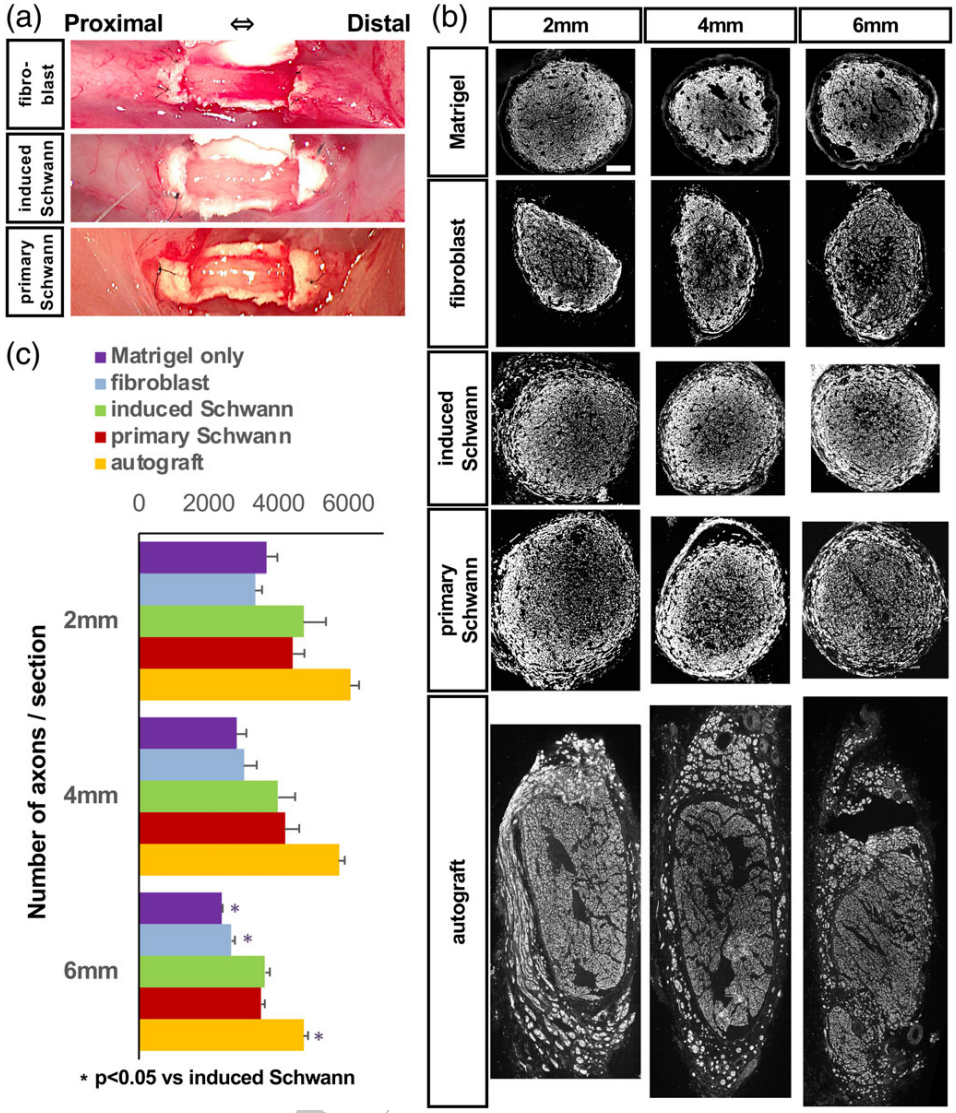

Color Figure - Print and Online

FIGURE 5 Promotion of axonal regeneration by induced Schwann cells after transplantation. (a) Macroscopic appearance of grafts 6 weeks after transplantation. Grafts containing fibroblasts (fibroblast), induced Schwann cells (induced Schwann), and primary human Schwann cells (primary Schwann) are shown. There seemed to be the tissue bridging the proximal and distal segments in each graft. Although the tissue inside the graft containing fibroblasts was reddish and vulnerable, the tissue inside grafts with induced Schwann cells or primary human Schwann cells looked whitish and solid. (b) Regenerating axons in the graft. Immunohistochemistry for neurofilament was performed using the transverse sections of grafts in the Matrigel-only (Matrigel), fibroblast (fibroblast), induced Schwann cell (induced Schwann), primary human Schwann cell (primary Schwann), or autograft (autograft) groups. (c) The number of neurofilament-positive axons in the transverse sections of grafts 2-, 4-, and 6-mm from the proximal end of each graft in the Matrigel-only (Matrigel), fibroblast (fibroblast), induced Schwann cells (induced Schwann), primary human Schwann cell (primary Schwann), and autograft (autograft) groups. The number of neurofilament-positive axons in induced Schwan cell group was significantly greater than those in the Matrigel-only and fibroblast groups at the 6-mm position (* $p < 0.05$), and was significantly lower than that in the autograft group only at the 6-mm position (*$p < 0.05$). Scale bar: (b), 200 μm

immunohistochemistry against MBP and neurofilament. The rate of myelination of regenerated axons in the inner area of the graft at the 6-mm position from the proximal end of the graft in the induced Schwann cell group (87.8 ± 0.47%) was similar to that in the primary human Schwann cell group (86.8 ± 2.06%), whereas that in the fibroblast group was statistically smaller (63.5 ± 2.53%) (Supporting Information Figure S4). In addition, GFP-positive transplanted cells containing MBP-positive myelin-like structure, in which neurofilament-positive axon-like structure was included, were detected in the grafts of the induced Schwann cell and primary human Schwann cell groups, not in that of the fibroblast group (Figure 6a). Furthermore, immunoelectron microscopy revealed myelination by the GFP-positive transplanted cells in the graft of the induced Schwann cell group (Figure 6b and Supporting Information Figure S5). These findings demonstrate that induced Schwann cells have the ability to myelinate regenerated axons after transplantation and suggest that the extent of the myelination ability is almost compatible to that of primary human Schwann cells.

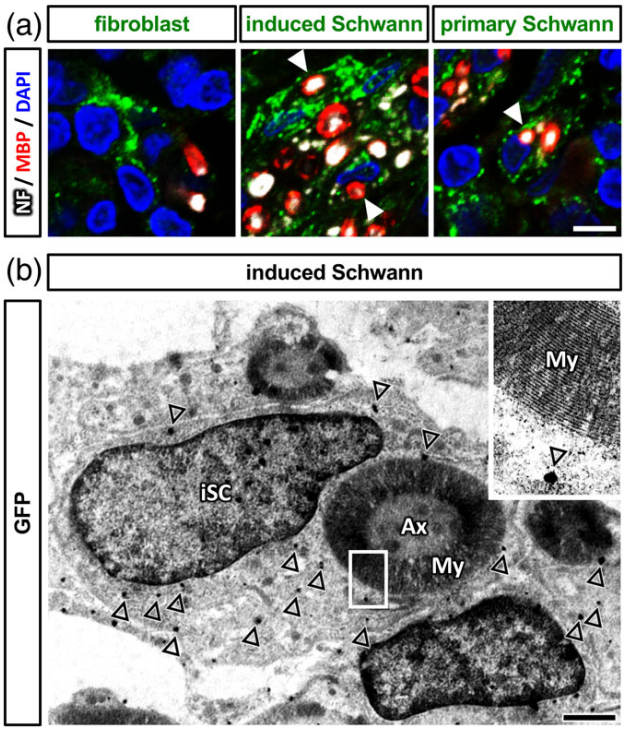

Color Figure - Print and Online

FIGURE 6 Myelination by induced Schwann cells after transplantation. (a) Immunostaining of the grafts at 6 weeks after transplantation. Immunohistochemistry against GFP (green), neurofilament (NF, white), and myelin basic protein (MBP, red) showed that, although there was no GFP-positive transplanted cell containing the MBP-positive myelin-like structures in the fibroblast group (fibroblast), some of the GFP-positive transplanted cells bore myelin-like structures positive for MBP, in which the neurofilament-positive axon was visible, in the sections of the induced Schwann cell (induced Schwann) and primary human Schwann cell (primary Schwann) groups (arrowheads). Nuclei were counterstained with DAPI (blue). (b) Immunoelectron microscopy of the section derived from an animal of the induced Schwann cell group (induced Schwann). GFP signals were labeled with silver enhanced-gold particles (open arrowheads). GFP-positive cells with myelinated axons were shown. Note that the myelin sheath was so tightly packed that silver-enhanced gold particles did not penetrate its center, but remained on the periphery of the sheath. Inset: The magnified image of the indicated rectangle. Abbreviations: iSC, induced Schwann cell; ax, axon; my, myelin. Scale bar: (a) 5 μm; (b) 1 μm

3.5 | Functional repair of the sciatic nerve after transplantation of induced Schwann cells

To evaluate the degree of functional recovery after transplantation of induced Schwann cells, we measured the SFI score every week for 6 weeks after transplantation (Figure 7). An SFI score of zero indicates normal function of the sciatic nerve, while a score of −100 means total dysfunction of the nerve (Bain et al., 1989; Varejao et al., 2001). An increase of the SFI score in the induced Schwann cell group was observed beginning at 2 weeks after transplantation, and the score gradually increased over the observation period. While the SFI score of the fibroblast group was almost the same as that of the Matrigel-only group at all time points, the score for the induced Schwann cell group was significantly higher than that in the Matrigel-only group at time points from 2 to 6 weeks after transplantation. Notably, no significant differences were observed between the scores of the induced Schwann cell and human Schwann cell groups over the observation period. The autograft group exhibited greater scores than any other groups, but there were no statistical differences compared with those observed in the induced Schwann cell group at any time points. These data demonstrate that induced Schwann cells can promote functional recovery of the severed peripheral nerve after transplantation and suggest that the degree of recovery is comparable to that from primary human Schwann cells.

3.6 | Re-formation of NMJs on the flexor digitorum brevis muscle

An improvement in SFI scores indicates that regenerated axons have reached flexor and extensor muscles on the affected side of the foot and re-formed NMJs to achieve well-coordinated movement of these muscles. We estimated re-formation of NMJs in the flexor digitorum brevis muscle, which is one of the important flexor muscles in the foot innervated with the sciatic nerve, and whose NMJs can be easily observed and evaluated after injury (Csillik, Nemcsok, Chase, Csillik, & Knyihar-Csillik, 1999). While the post-synaptic side of NMJs can be detected by α-bungarotoxin, which binds to the nicotinic acetylcholine receptor (AchR), the spread localization or even ectopic expression of AchR were reported after denervation caused by complete transection of the sciatic nerve (Csillik et al., 1999). For a precise evaluation of NMJ re-formation, we performed immunohistochemistry to detect synaptophysin on the pre-synapse side of NMJs, and then applied α-bungarotoxin to detect the posy-synaptic side (Figure 8a). Analysis of the number of NMJs that were double positive for synaptophysin and α-bungarotoxin in the flexor digitorum brevis muscle of each transplanted group 6 weeks after transplantation revealed that there was a greater number of NMJs in the induced Schwann cell group than in either the Matrigel-only or fibroblast groups. The number of NMJs did not significantly differ between the induced Schwann cell and primary human Schwann cell groups (Figure 8b). Also, there was no statistical difference in the autograft and induced Schwann cell group. These findings indicate that induced Schwann cells can efficiently promote re-formation of NMJs at nearly the same level as transplanted primary human Schwann cells.

3.7 | The mechanisms of axonal regeneration in the Matrigel and fibroblast groups

Although the numbers of neurofilament-positive axons in the Matrigel-only and fibroblast groups were consistently lesser than those in the induced Schwann cells group, there were no statistical differences between these groups at the 2- and 4-mm positions. In addition, there was no statistical difference in the numbers of neurofilament-positive axons between the Matrigel-only and fibroblast groups at all three positions. These findings indicate that fibroblasts do not substantially contribute to regeneration of axons in the peripheral nerve injury model used in this study and suggest that Matrigel itself facilitates axonal regeneration. To approach the mechanisms of axonal regeneration in the Matrigel-only and fibroblast

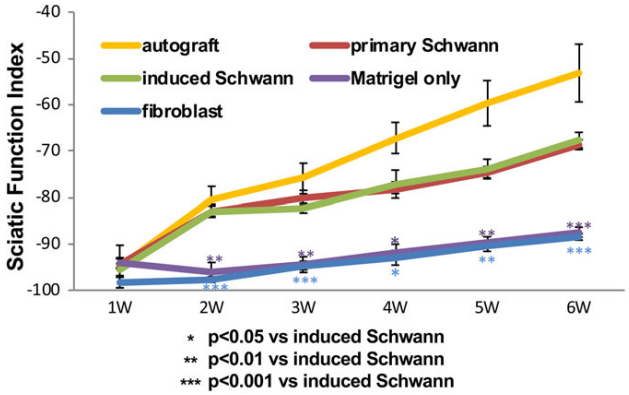

FIGURE 7 Recovery of sciatic nerve function in the induced Schwann cell group. Walking track analysis based on the sciatic function index (SFI) score evaluated up to 6 weeks after transplantation. SFI scores from 2 to 6 weeks were significantly improved in the induced Schwann cell (induced Schwann) and primary human Schwann cell (primary Schwann) groups compared with the fibroblast (fibroblast) and Matrigel-only groups. There were no significant differences in scores between the induced Schwann cell and primary human Schwann cell groups over the observation period. Also, the fibroblast group showed no significant differences from the Matrigel-only group. The autograft group showed better scores than any other groups, but no statistical differences were detected in the SFI scores between the autograft and induced Schwann cell groups at any time points

groups, we observed the fine structure of the graft of the fibroblast group (Supporting Information Figure S6). We found small vessels, in which an endothelial cell intimately contacted to a Schwann cell through the basement membrane in the outer are of the graft at the 6-mm position (Supporting Information Figure S6A), suggesting the migration of Schwann cells on the newly formed vessels, which enhanced axonal regeneration (Cattin et al., 2015). In the outer area, there were many myelinated axons and mature Schwann cells tightly packed within the cellular processes of fibroblasts, indicating the mature re-constructed nerve tissue (data not shown). However, we also found the loose area lacking vessels, where there were many unmyelinated axons in addition to myelinated axons both wrapped by Schwann cells in the inner area of the graft at the 6-mm position (Supporting Information Figure S6B), suggesting immature re-constructing nerve tissue. In such loose area, extracellular matrices were obviously observed. These findings imply that host Schwann cells of the proximal end of the host nerve initially migrate into the graft, tracing on the surface of newly formed vessels to facilitate and support axonal regeneration in the outer area of the graft, enabling the relatively fast re-construction of nerve tissue, whereas such vessel-assisted Schwann cell migration mechanism does not impact on axonal regeneration in the inner area of the graft and axons relatively slowly regenerate, being guided by Schwann cells driven by extracellular matrices and trophic factors derived from Matrigel.

3.8 | The character of adult human skin fibroblasts

To characterize the adult human skin fibroblasts used in this study, we analyzed the cell surface antigen expression by flow cytometry (Supporting Information Figure S7). Most of them expressed CD44, CD73, and CD90, whereas they did not express CD34 and CD45 on their cellular surface, showing the mesenchymal character of this cell population and no contamination of blood cells. Since these cell

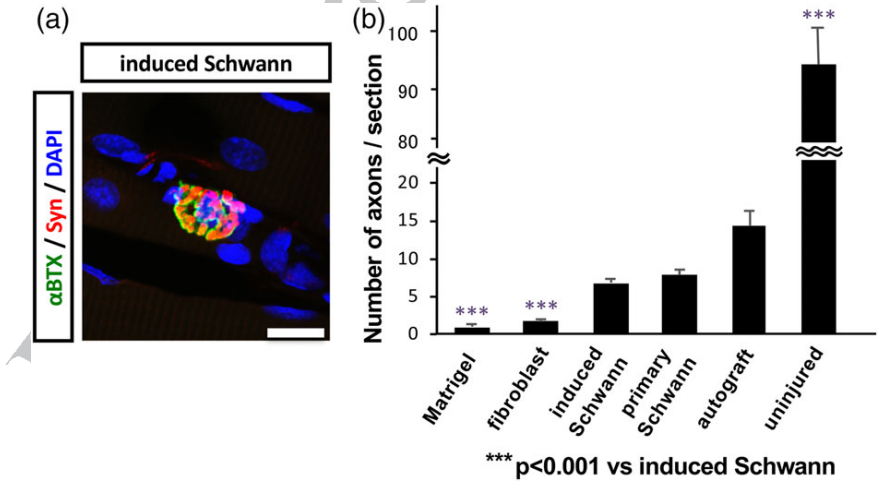

FIGURE 8 Re-formation of neuromuscular junctions (NMJs) by induced Schwann cells after transplantation. (a) An example of NMJs on the flexor digitorum brevis muscle. Pre- and post-synaptic sites were detected by immunohistochemistry for synaptophysin (Syn, red) and by α-bungarotoxin (αBTX, green) for acetylcholine receptor. Nuclei were counterstained with DAPI (blue). (b) The number of NMJs in a 10-μm-thick cryosection. The higher number of NMJs was observed in the induced Schwann cell (induced Schwann) and primary Schwan cell (primary Schwann) groups compared with that of the Matrigel-only (Matrigel) and fibroblast (fibroblast) groups. The number of NMJs did not significantly differ between the induced Schwann cell and primary human Schwann cell groups. The number of NMJs in the induced Schwann cells was significantly higher than those in the Matrigel-only and fibroblast groups (***$p < 0.001$). The autograft group (autograft) showed a greater number of NMJs, but there was no statistical difference in the autograft and induced Schwann cell group. The uninjured animal group (uninjured) exhibited the highest number of NMJs among all the groups, which was significantly higher than that in induced Schwann cell group ($p < 0.001$). Scale bar: (a), 20 μm

surface expression pattern of adult fibroblasts has been also reported in many previous studies (Blasi et al., 2011; Itoh et al., 2013), our method for Schwann cell induction from human adult skin fibroblasts is considered applied to other regular human fibroblasts.

There is a concern that adult human skin fibroblasts used in this study contain a very low percentage of stem/progenitor cell populations, which can produce Schwann cells under the differentiation mechanism but not through direct reprogramming. To assess this possibility, we evaluated the contamination of such cell populations by flow cytometry (Figure 9). There are small populations, which expressed CD271 (a cell surface marker of neural crest-derived stem cells) (Nagoshi et al., 2008), CD117 (melanoblasts) (Nishimura et al., 2002), or Stage-specific embryonic antigen-3 (SSEA-3) (multilineage-differentiating stress enduring cells) (Kuroda et al., 2010; 2013) (Figure 9a), showing the existence of putative stem/progenitor cell populations in the adult human skin fibroblast culture. To exclude the possibility that these putative stem/progenitor populations mainly contributed to the production of Schwann cells from human fibroblasts, we collected the cell population triple-negative for CD271, CD117, and SSEA-3 from adult human skin fibroblasts by FACS to induce Schwann cells. After the sequential treatments with chemical agents and trophic factors, Schwann cells were successfully induced from the triple-negative cell population (Figure 9b). The rate of p75-positive cells was 71.1 ± 5.34%, similar to that was calculated with induced Schwann cells derived from whole cultured cells of adult human skin fibroblasts. These findings clearly demonstrate that stem/progenitor cells rarely contaminated in the fibroblast culture were not the principal cell source of induced Schwann cells and that the differentiation from these cells is not the main mechanism of Schwann cell induction demonstrated in this study.

4 | DISCUSSION

Stably proliferating, easily accessible adult human skin fibroblasts can be converted into cells comparable to authentic human Schwann cells by an optimized induction system that was initially developed for trans-differentiation from MSCs. The efficiency of conversion was suggested to be approximately 75%, evaluated by the Schwann cell marker expression. Transplantation of induced Schwann cells into a rat sciatic nerve injury model facilitated axonal regrowth and functional recovery to nearly the same extent as those observed following transplantation of primary human Schwann cells. The contributions of induced Schwann cells to myelination of regenerated axons and reformation of NMJs were also confirmed. This is the first report to indicate that a large number of Schwann cells, which mediate functional recovery after transplantation into a PNS injury model, can be readily obtained from easily accessible adult human skin fibroblasts without gene introduction.

4.1 | Functional recovery by induced Schwann cells

Functional recovery of the transected sciatic nerve is known to be achieved only when all the following requirements are met: (1) axons re-grow from the proximal side of the transected nerve segment and penetrate into the distal side of the nerve, (2) regenerated axons become myelinated, (3) axons reach the target muscles, and (4) NMJs are re-formed (Allodi et al., 2012). We found, by measurement of neurofilament-positive signals in the graft and SFI scores at 6 weeks after transplantation, that the induced Schwann cell group showed neuro-regenerative activity comparable to that in the primary human Schwann cell group and that functional recovery was significantly more efficient in these groups than in the fibroblast group. We also

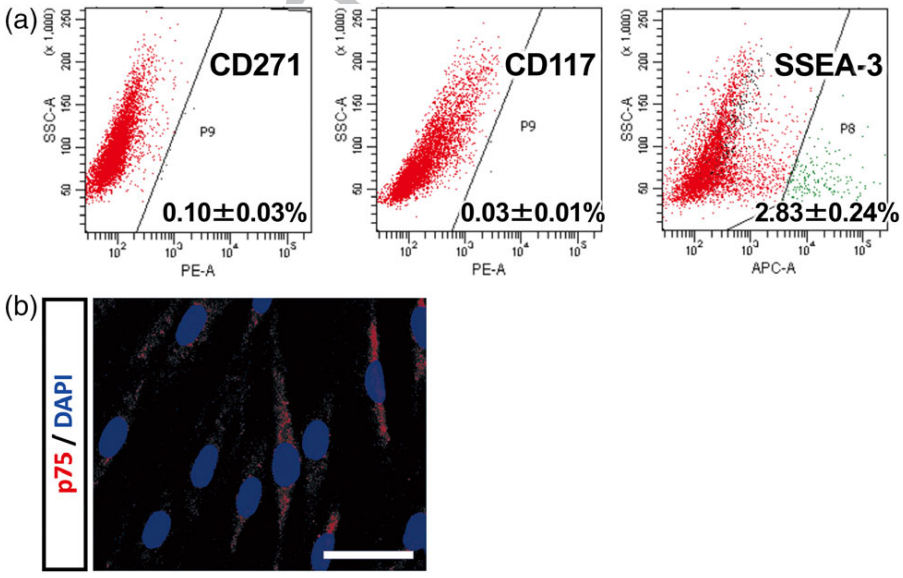

Color Figure - Print and Online

FIGURE 9 The contribution of putative stem/progenitor cell populations in Schwann cell induction. (a) Flow cytometry analysis for stem/progenitor cell populations that were contained in adult human skin fibroblasts. They contained small populations expressing CD271 (neural crest-derived stem cell marker), CD117 (melanoblast marker), or stage-specific embryonic antigen-3 (SSEA-3, multilineage-differentiating stress enduring cell marker). (b) Schwann cells induced from the FACS-sorted cell population triple negative for CD271, CD117, and SSEA-3 expressed p75 (red). Scale bar: (b), 50 μm

demonstrated the formation of myelin and re-formation of NMJs by transplanted induced Schwann cells. Collectively, these findings indicate that transplanted adult human skin fibroblasts-derived Schwann cells contribute to each of the four steps outlined above to achieve functional recovery of a transected peripheral nerve.

In this study, we showed that transplanted induced Schwann cells and primary human Schwann cells significantly promoted re-formation of NMJs on the flexor digitorum brevis muscle compared with transplanted fibroblasts. However, the sites of NMJs on the target muscles of regenerating axons were quite distant from that of the transplantation, so that it was not conceivable that transplanted Schwann cells migrated to the sites of NMJs to promote their re-formation. This raises the question: What is the mechanism of re-formation of NMJs by transplanted Schwann cells? Recent studies have shown that Schwann cell-conditioned medium promotes formation of NMJs in *Xenopus* and rats, where transforming growth factor beta-1 (TGF-ß1) plays a pivotal role (Feng & Ko, 2008a, 2008b). The signal of TGF-ß1 secreted by Schwann cells is mediated by its receptor, TGF receptor type II, which localizes to the axonal membrane of spinal neurons (Jiang, McLennan, Koishi, & Hendry, 2000). With the TGF-ß1 signaling, neurons synthesize and secrete agrin, a heparan sulfate proteoglycan that is indispensable for synaptogenesis (Gautam et al., 1996), and stimulate the aggregation of AchR in the post-synaptic membrane to promote synaptogenesis (Reist, Werle, & McMahan, 1992). This TGF-ß1-mediated agrin secretion mechanism might account for the enhancement of NMJ re-formation observed in the present study.

A variety of neural diseases, both in and CNS including traumatic neural injuries, including peripheral nerve injury, optic nerve injury, and spinal cord injury, as well as demyelinating diseases such as multiple sclerosis, could be targets of Schwann cell-based therapies (Aguayo et al., 1981; Baron-Van Evercooren et al., 1997; Dezawa et al., 1997; Lavdas et al., 2008; Martin et al., 1996; Zujovic et al., 2012). Using a simple method and in a relatively short period of time, our system enabled obtaining a large number of functional Schwann cells applicable to the treatment of various neural injuries and diseases mentioned above from easily accessible adult human skin fibroblasts.

4.2 | The function of induced Schwann cells as regenerative cells in the peripheral nerve injury

In the peripheral nerve after injury, myelin-forming mature Schwann cells has been considered to de-differentiate into an earlier stage resembling the immature Schwann cells of perinatal nerves. Recent studies have proposed a novel insight that Schwann cells do not de-differentiate but trans-differentiate into regenerative cells namely Bungner cells, where a transcription factor c-Jun reprograms Schwann cells into Bungner cells and governs the response to injury to support regeneration of axons and survival of neurons and regulate autophagy of myelin (myelinophagy), the clearance of myelin, and the activity of macrophages (Arthur-Farraj et al., 2012; Fontana et al., 2012; Gomez-Sanchez et al., 2015; Jessen & Mirsky, 2016; Jessen, Mirsky, & Lloyd, 2015). This transcription factor sequentially activates the repair programs: (1) the secretion of trophic factors including glial cell line-derived neurotrophic factor, artemin, and brain-derived neurotrophic factor and the expression of cell surface proteins such as p75 and N-cadherin in direct and indirect manners to support survival of neurons and axonal growth; (2) the exertion of myelinophagy to initiate the clearance of myelin; and (3) the construction of the regeneration tracks namely Bungner bands to facilitate regeneration of axons. In the present study, we only demonstrated the potential of induced Schwann cells in terms of enhancing axonal regeneration at an extent compatible to that of primary human Schwann cells. Further studies will elucidate whether Schwann cells induced from adult human skin fibroblasts can exert any other functions of Bungner cells in peripheral nerve repair such as the regulation of survival of neurons, myelinophagy, the clearance of myelin, and the activity of macrophages.

4.3 | Merits of the Schwann cell induction system used in this study

As we originally developed this induction system for trans-differentiation of bone marrow MSCs into Schwann cells, many studies, including ours and those of other research groups, have demonstrated that this system is valid for the trans-differentiation of MSCs from many kinds of tissues, including bone marrow, adipose tissue, and umbilical cord (Kingham et al., 2007; Peng et al., 2011; Tohill et al., 2004) from various animal species such as rats, rabbits, monkeys, and humans (Lu et al., 2008; Wakao et al., 2010; Wang et al., 2011; Xu et al., 2008) into Schwann cells. This induction system is highly efficient, with more than 95% of MSCs trans-differentiating into Schwann cells that can support axonal regeneration and myelinate regenerated axons to achieve functional recovery in the PNS and CNS after transplantation (Dezawa et al., 2001; Kamada et al., 2005). In addition, the safety of this induction system has already been demonstrated by a one-year observational study, which confirmed the lack of toxicity and tumorigenesis. Safety was evaluated by monitoring the general condition, cell proliferation, and positron emission tomography with fludeoxyglucose of a primate model of PNS injury after autologous transplantation of the Schwann cells (Wakao et al., 2010). In addition, many modifications of this induction system have been reported. In the present study, we evaluated this induction system for direct conversion of adult human skin fibroblasts into Schwann cells and demonstrated the successful induction of functional Schwann cells, which facilitated functional recovery of the severed PNS nerve after transplantation, by supporting axonal regeneration, myelination of regenerated axons, and re-formation of NMJs at a level comparable to those seen with primary human Schwann cells.

Thus, the merits of this Schwann cell induction system mentioned above are expected to be also applicable to adult human fibroblasts, and this induction system may serve as a practical tool for direct conversion of fibroblasts into Schwann cells for clinical use.

4.4 | The character of induced Schwann cells

In this study, we performed genome-wide gene expression profiling by RNA-seq (Figure 4 and Supporting Information Figure S3). The heatmap and clustering analysis showed that induced Schwann cells exhibited some aspects of the characteristics of mesenchymal cells, however, gene set enrichment analysis demonstrated the down-regulation of the development and function of mesenchymal cells. On

the other hand, up-regulation of the cell signaling-associated gene sets for Wnt, bFGF, BMP, and TGF-beta were confirmed. The cell signaling of Wnt, bFGF, and BMP are known to induce the neural crest-lineage cells (Villanueva et al., 2002), and TGF-beta signaling is reported to induce cell proliferation and block myelin gene expression in Schwann cells and their precursors (Jacob et al., 2008; Stewart et al., 1995). In addition, the expression profile of the cell cycle-associated gene set implies the proliferation potential of induced Schwann cells might be lower than fibroblasts but higher than primary human Schwann cells (Supporting Information Figure S3C). Well-known, the proliferation potential of primary human Schwann cells is much lower than that of fibroblasts, so that cytosine arabinoside is typically used for the elimination of contaminating fibroblasts in primary human Schwann cell culture (Brockes, Fields, & Raff, 1979). As mentioned, there are many reports for the modification of the Schwann cell induction system, where authors pointed out a possibility of immaturity of mesenchymal cell-derived Schwann cells induced by our original method (Gao et al., 2015; Liu et al., 2016). Gao et al. reported that the treatment with dihydrotestosterone after the treatment of the original protocol increased the mRNA level of S100 and P0 (Gao et al., 2015), and Liu et al. supplemented progesterone, hydrocortisone, and insulin to the cocktail of trophic factors used in this study to elucidate that phenotypically more mature Schwann cells were induced (Liu et al., 2016). The results of such studies and the findings in the present study suggest that induced Schwann cells in the present study are relatively immature than primary human Schwann cells or rather might have more similarities to Schwann cell precursors. Indeed, we could not obtain the solid data of in vitro myelination of neurites of PC12 cells by induced Schwann cells (data not shown). Better protocols to facilitate the maturation of induced Schwann cells might have led the successful in vitro myelination. However, even if they were immature in vitro, they could enhance the regeneration of axons and myelinate them to improve functional repair after transplantation into the damaged peripheral nerve, where the extent of morphological and functional repair was almost compatible to that observed after transplantation of primary human Schwann cells. These findings collectively implied that the further treatment for the in vitro maturation of induced Schwann cells may not be necessary prior to the transplantation.

4.5 | Fibroblasts as a feasible cell source for regenerative medicine

MSCs can differentiate into many kinds of tissue-specific cells; therefore, they have been a focus of research on cell therapies for replenishing lost cells. In addition, MSCs derived from bone marrow and adipose tissue can be harvested directly from patients. However, invasive procedures such as bone marrow aspiration and liposuction are required for collecting MSCs. Also, the use of the umbilical cord as a source of MSCs gives concerns such as limited supply. Although there are some studies that have shown the multi-potentiality of fibroblasts (Dastagir et al., 2014; Sudo et al., 2007), these cells are generally considered to be differentiated, so that, unlike MSCs, their differentiation potential is not considered sufficient for clinical application (Brohem et al., 2013). In contrast, fibroblasts can be harvested from the skin much more easily than MSCs, and, similar to MSCs, they can be collected from the patient without ethical concerns. In addition, they are one of the most widely distributed, commercially available human cell lines, and they can be readily expanded for clinical and industrial use. If it is possible to obtain the needed cells by direct conversion from fibroblasts without gene transfer, they will be considered one of the most promising cell sources for clinical application. In this study, we demonstrated direct reprogramming of fibroblasts into functional Schwann cells without gene transfer. Recent studies have shown that a certain type of tissue cell, namely neurons, can be induced with direct conversion methods using only a cocktail of small molecules (Hu et al., 2015; Li et al., 2015), further suggesting the possibility that the cells on demand are obtainable by direct conversion without gene transfer. Thus, fibroblasts will be broadly utilized as a realistic cell source for clinical applications.

ACKNOWLEDGMENTS

This work was supported by a Health Labor Sciences Research Grant from the Ministry of Health, Labor, and Welfare, Japan (MD), and a Grant-in-Aid for Research Activity Start-up, Japan Society for the Promotion of Science (TM). GENEWIZ helped next generation sequencing and analysis of RNA-seq data. Editage (http://www.editage.com) helped authors with English editing and proofreading of this manuscript.

CONFLICT OF INTEREST

There is no conflict of interest.

ORCID

Toru Murakami https://orcid.org/0000-0002-6947-6328

REFERENCES

Aguayo, A. J., David, S., & Bray, G. M. (1981). Influences of the glial environment on the elongation of axons after injury: Transplantation studies in adult rodents. *Journal of Experimental Biology*, *95*, 231–240.

Allodi, I., Udina, E., & Navarro, X. (2012). Specificity of peripheral nerve regeneration: Interactions at the axon level. *Progress in Neurobiology*, *98*(1), 16–37. https://doi.org/10.1016/j.pneurobio.2012.05.005

Arthur-Farraj, P. J., Latouche, M., Wilton, D. K., Quintes, S., Chabrol, E., Banerjee, A., … Jessen, K. R. (2012). C-Jun reprograms Schwann cells of injured nerves to generate a repair cell essential for regeneration. *Neuron*, *75*(4), 633–647. https://doi.org/10.1016/j.neuron.2012.06.021

Bain, J. R., Mackinnon, S. E., & Hunter, D. A. (1989). Functional evaluation of complete sciatic, peroneal, and posterior tibial nerve lesions in the rat. *Plastic and Reconstructive Surgery*, *83*(1), 129–138.

Baron-Van Evercooren, A., Avellana-Adalid, V., Lachapelle, F., & Liblau, R. (1997). Schwann cell transplantation and myelin repair of the CNS. *Multiple Sclerosis*, *3*(2), 157–161.

Blasi, A., Martino, C., Balducci, L., Saldarelli, M., Soleti, A., Navone, S. E., … Alessandri, G. (2011). Dermal fibroblasts display similar phenotypic and differentiation capacity to fat-derived mesenchymal stem cells, but differ in anti-inflammatory and angiogenic potential. *Vascular Cell*, *3*(1), 5. https://doi.org/10.1186/2045-824X-3-5

Brockes, J. P., Fields, K. L., & Raff, M. C. (1979). Studies on cultured rat Schwann cells. I. Establishment of purified populations from cultures of peripheral nerve. *Brain Research*, *165*(1), 105–118.

Brohem, C. A., de Carvalho, C. M., Radoski, C. L., Santi, F. C., Baptista, M. C., Swinka, B. B., … Lorencini, M. (2013). Comparison

between fibroblasts and mesenchymal stem cells derived from dermal and adipose tissue. *International Journal of Cosmetic Science*, *35*(5), 448–457. https://doi.org/10.1111/ics.12064

Cattin, A. L., Burden, J. J., Van Emmenis, L., Mackenzie, F. E., Hoving, J. J., Garcia Calavia, N., … Lloyd, A. C. (2015). Macrophage-induced blood vessels guide Schwann cell-mediated regeneration of peripheral nerves. *Cell*, *162*(5), 1127–1139. https://doi.org/10.1016/j.cell.2015.07.021

Csillik, B., Nemcsok, J., Chase, B., Csillik, A. E., & Knyihar-Csillik, E. (1999). Infraterminal spreading and extrajunctional expression of nicotinic acetylcholine receptors in denervated rat skeletal muscle. *Experimental Brain Research*, *125*(4), 426–434.

Dastagir, K., Reimers, K., Lazaridis, A., Jahn, S., Maurer, V., Strauss, S., … Vogt, P. M. (2014). Murine embryonic fibroblast cell lines differentiate into three mesenchymal lineages to different extents: New models to investigate differentiation processes. *Cellular Reprogramming*, *16*(4), 241–252. https://doi.org/10.1089/cell.2014.0005

Dezawa, M., Kawana, K., & Adachi-Usami, E. (1997). The role of Schwann cells during retinal ganglion cell regeneration induced by peripheral nerve transplantation. *Investigative Ophthalmology and Visual Science*, *38*(7), 1401–1410.

Dezawa, M., Takahashi, I., Esaki, M., Takano, M., & Sawada, H. (2001). Sciatic nerve regeneration in rats induced by transplantation of in vitro differentiated bone-marrow stromal cells. *European Journal of Neuroscience*, *14*(11), 1771–1776.

Dong, Z., Sinanan, A., Parkinson, D., Parmantier, E., Mirsky, R., & Jessen, K. R. (1999). Schwann cell development in embryonic mouse nerves. *Journal of Neuroscience Research*, *56*(4), 334–348.

Feng, Z., & Ko, C. P. (2008a). The role of glial cells in the formation and maintenance of the neuromuscular junction. *Annals of the New York Academy of Sciences*, *1132*, 19–28. https://doi.org/10.1196/annals.1405.016

Feng, Z., & Ko, C. P. (2008b). Schwann cells promote synaptogenesis at the neuromuscular junction via transforming growth factor-beta1. *Journal of Neuroscience*, *28*(39), 9599–9609. https://doi.org/10.1523/JNEUROSCI.2589-08.2008

Finzsch, M., Schreiner, S., Kichko, T., Reeh, P., Tamm, E. R., Bosl, M. R., … Wegner, M. (2010). Sox10 is required for Schwann cell identity and progression beyond the immature Schwann cell stage. *Journal of Cell Biology*, *189*(4), 701–712. https://doi.org/10.1083/jcb.200912142

Fontana, X., Hristova, M., Da Costa, C., Patodia, S., Thei, L., Makwana, M., … Behrens, A. (2012). C-Jun in Schwann cells promotes axonal regeneration and motoneuron survival via paracrine signaling. *The Journal of Cell Biology*, *198*(1), 127–141. https://doi.org/10.1083/jcb.201205025

Gao, S., Zheng, Y., Cai, Q., Wu, X., Yao, W., & Wang, J. (2015). Different methods for inducing adipose-derived stem cells to differentiate into Schwann-like cells. *Archives of Medical Science*, *11*(4), 886–892. https://doi.org/10.5114/aoms.2015.53310

Garbay, B., Heape, A. M., Sargueil, F., & Cassagne, C. (2000). Myelin synthesis in the peripheral nervous system. *Progress in Neurobiology*, *61*(3), 267–304.

Garratt, A. N., Britsch, S., & Birchmeier, C. (2000). Neuregulin, a factor with many functions in the life of a schwann cell. *BioEssays*, *22*(11), 987–996. https://doi.org/10.1002/1521-1878(200011)22:11<987::AID-BIES5>3.0.CO;2-5

Gautam, M., Noakes, P. G., Moscoso, L., Rupp, F., Scheller, R. H., Merlie, J. P., & Sanes, J. R. (1996). Defective neuromuscular synaptogenesis in agrin-deficient mutant mice. *Cell*, *85*(4), 525–535.

Gomez-Sanchez, J. A., Carty, L., Iruarrizaga-Lejarreta, M., Palomo-Irigoyen, M., Varela-Rey, M., Griffith, M., … Jessen, K. R. (2015). Schwann cell autophagy, myelinophagy, initiates myelin clearance from injured nerves. *The Journal of Cell Biology*, *210*(1), 153–168. https://doi.org/10.1083/jcb.201503019

Grigoryan, T., & Birchmeier, W. (2015). Molecular signaling mechanisms of axon-glia communication in the peripheral nervous system. *BioEssays*, *37*(5), 502–513. https://doi.org/10.1002/bies.201400172

Haack, H., & Hynes, R. O. (2001). Integrin receptors are required for cell survival and proliferation during development of the peripheral glial lineage. *Developmental Biology*, *233*(1), 38–55. https://doi.org/10.1006/dbio.2001.0213

Hacein-Bey-Abina, S., Von Kalle, C., Schmidt, M., Le Deist, F., Wulffraat, N., McIntyre, E., … Fischer, A. (2003). A serious adverse event after successful gene therapy for X-linked severe combined immunodeficiency. *New England Journal of Medicine*, *348*(3), 255–256. https://doi.org/10.1056/NEJM200301163480314

Hacein-Bey-Abina, S., Von Kalle, C., Schmidt, M., McCormack, M. P., Wulffraat, N., Leboulch, P., … Cavazzana-Calvo, M. (2003). LMO2-associated clonal T cell proliferation in two patients after gene therapy for SCID-X1. *Science*, *302*(5644), 415–419. https://doi.org/10.1126/science.1088547

Hu, W., Qiu, B., Guan, W., Wang, Q., Wang, M., Li, W., … Pei, G. (2015). Direct conversion of Normal and Alzheimer's disease human fibroblasts into neuronal cells by small molecules. *Cell Stem Cell*, *17*(2), 204–212. https://doi.org/10.1016/j.stem.2015.07.006

Itoh, M., Umegaki-Arao, N., Guo, Z., Liu, L., Higgins, C. A., & Christiano, A. M. (2013). Generation of 3D skin equivalents fully reconstituted from human induced pluripotent stem cells (iPSCs). *PLoS One*, *8*(10), e77673. https://doi.org/10.1371/journal.pone.0077673

Jacob, C., Grabner, H., Atanasoski, S., & Suter, U. (2008). Expression and localization of ski determine cell type-specific TGFbeta signaling effects on the cell cycle. *Journal of Cell Biology*, *182*(3), 519–530. https://doi.org/10.1083/jcb.200710161

Jessen, K. R., Brennan, A., Morgan, L., Mirsky, R., Kent, A., Hashimoto, Y., & Gavrilovic, J. (1994). The Schwann cell precursor and its fate: A study of cell death and differentiation during gliogenesis in rat embryonic nerves. *Neuron*, *12*(3), 509–527.

Jessen, K. R., & Mirsky, R. (2005). The origin and development of glial cells in peripheral nerves. *Nature Reviews: Neuroscience*, *6*(9), 671–682. https://doi.org/10.1038/nrn1746

Jessen, K. R., & Mirsky, R. (2016). The repair Schwann cell and its function in regenerating nerves. *The Journal of Physiology*, *594*(13), 3521–3531. https://doi.org/10.1113/JP270874

Jessen, K. R., Mirsky, R., & Lloyd, A. C. (2015). Schwann cells: Development and role in nerve repair. *Cold Spring Harbor Perspectives in Biology*, *7*(7), a020487. https://doi.org/10.1101/cshperspect.a020487

Jessen, K. R., Morgan, L., Stewart, H. J., & Mirsky, R. (1990). Three markers of adult non-myelin-forming Schwann cells, 217c(Ran-1), A5E3 and GFAP: Development and regulation by neuron-Schwann cell interactions. *Development*, *109*(1), 91–103.

Jiang, Y., McLennan, I. S., Koishi, K., & Hendry, I. A. (2000). Transforming growth factor-beta 2 is anterogradely and retrogradely transported in motoneurons and up-regulated after nerve injury. *Neuroscience*, *97*(4), 735–742.

Joseph, N. M., Mukouyama, Y. S., Mosher, J. T., Jaegle, M., Crone, S. A., Dormand, E. L., … Morrison, S. J. (2004). Neural crest stem cells undergo multilineage differentiation in developing peripheral nerves to generate endoneurial fibroblasts in addition to Schwann cells. *Development*, *131*(22), 5599–5612. https://doi.org/10.1242/dev.01429

Kamada, T., Koda, M., Dezawa, M., Yoshinaga, K., Hashimoto, M., Koshizuka, S., … Yamazaki, M. (2005). Transplantation of bone marrow stromal cell-derived Schwann cells promotes axonal regeneration and functional recovery after complete transection of adult rat spinal cord. *Journal of Neuropathology and Experimental Neurology*, *64*(1), 37–45.

Kim, Y. J., Lim, H., Li, Z., Oh, Y., Kovlyagina, I., Choi, I. Y., … Lee, G. (2014). Generation of multipotent induced neural crest by direct reprogramming of human postnatal fibroblasts with a single transcription factor. *Cell Stem Cell*, *15*(4), 497–506. https://doi.org/10.1016/j.stem.2014.07.013

Kingham, P. J., Kalbermatten, D. F., Mahay, D., Armstrong, S. J., Wiberg, M., & Terenghi, G. (2007). Adipose-derived stem cells differentiate into a Schwann cell phenotype and promote neurite outgrowth in vitro. *Experimental Neurology*, *207*(2), 267–274. https://doi.org/10.1016/j.expneurol.2007.06.029

Kitada, M., Chakrabortty, S., Matsumoto, N., Taketomi, M., & Ide, C. (2001). Differentiation of choroid plexus ependymal cells into astrocytes after grafting into the pre-lesioned spinal cord in mice. *Glia*, *36*(3), 364–374.

Kitada, M., & Dezawa, M. (2009). Induction system of neural and muscle lineage cells from bone marrow stromal cells; a new strategy for tissue reconstruction in degenerative diseases. *Histology and Histopathology*, *24*(5), 631–642.

Kuroda, Y., Kitada, M., Wakao, S., & Dezawa, M. (2011). Bone marrow mesenchymal cells: How do they contribute to tissue repair and are they really stem cells? *Archivum Immunologiae et Therapiae Experimentalis*, *59*(5), 369–378. https://doi.org/10.1007/s00005-011-0139-9

Kuroda, Y., Kitada, M., Wakao, S., Nishikawa, K., Tanimura, Y., Makinoshima, H., … Dezawa, M. (2010). Unique multipotent cells in adult human mesenchymal cell populations. *Proceedings of the National Academy of Sciences of the United States of America*, *107*(19), 8639–8643. https://doi.org/10.1073/pnas.0911647107

Kuroda, Y., Wakao, S., Kitada, M., Murakami, T., Nojima, M., & Dezawa, M. (2013). Isolation, culture and evaluation of multilineage-differentiating stress-enduring (muse) cells. *Nature Protocols*, *8*(7), 1391–1415. https://doi.org/10.1038/nprot.2013.076

Lavdas, A. A., Papastefanaki, F., Thomaidou, D., & Matsas, R. (2008). Schwann cell transplantation for CNS repair. *Current Medicinal Chemistry*, *15*(2), 151–160.

Lee, M., Brennan, A., Blanchard, A., Zoidl, G., Dong, Z., Tabernero, A., … Mirsky, R. (1997). P0 is constitutively expressed in the rat neural crest and embryonic nerves and is negatively and positively regulated by axons to generate non-myelin-forming and myelin-forming Schwann cells, respectively. *Molecular and Cellular Neurosciences*, *8*(5), 336–350.

Li, X., Zuo, X., Jing, J., Ma, Y., Wang, J., Liu, D., … Deng, H. (2015). Small-molecule-driven direct reprogramming of mouse fibroblasts into functional neurons. *Cell Stem Cell*, *17*(2), 195–203. https://doi.org/10.1016/j.stem.2015.06.003

Liu, Y., Chen, J., Liu, W., Lu, X., Liu, Z., Zhao, X., … Chen, Z. (2016). A modified approach to inducing bone marrow stromal cells to differentiate into cells with mature Schwann cell phenotypes. *Stem Cells and Development*, *25*(4), 347–359. https://doi.org/10.1089/scd.2015.0295

Livak, K. J., & Schmittgen, T. D. (2001). Analysis of relative gene expression data using real-time quantitative PCR and the 2(−Delta Delta C [T]) method. *Methods*, *25*(4), 402–408. https://doi.org/10.1006/meth.2001.1262

Lu, L., Chen, X., Zhang, C. W., Yang, W. L., Wu, Y. J., Sun, L., … Xiao, Z. C. (2008). Morphological and functional characterization of predifferentiation of myelinating glia-like cells from human bone marrow stromal cells through activation of F3/notch signaling in mouse retina. *Stem Cells*, *26*(2), 580–590. https://doi.org/10.1634/stemcells.2007-0106

Martin, D., Robe, P., Franzen, R., Delree, P., Schoenen, J., Stevenaert, A., & Moonen, G. (1996). Effects of Schwann cell transplantation in a contusion model of rat spinal cord injury. *Journal of Neuroscience Research*, *45*(5), 588–597. https://doi.org/10.1002/(SICI)1097-4547(19960901)45:5<588::AID-JNR8>3.0.CO;2–8

Matsuse, D., Kitada, M., Kohama, M., Nishikawa, K., Makinoshima, H., Wakao, S., … Dezawa, M. (2010). Human umbilical cord-derived mesenchymal stromal cells differentiate into functional Schwann cells that sustain peripheral nerve regeneration. *Journal of Neuropathology and Experimental Neurology*, *69*(9), 973–985. https://doi.org/10.1097/NEN.0b013e3181eff6dc

Mirsky, R., Woodhoo, A., Parkinson, D. B., Arthur-Farraj, P., Bhaskaran, A., & Jessen, K. R. (2008). Novel signals controlling embryonic Schwann cell development, myelination and dedifferentiation. *Journal of the Peripheral Nervous System*, *13*(2), 122–135. https://doi.org/10.1111/j.1529-8027.2008.00168.x

Mitchell, P. J., Timmons, P. M., Hebert, J. M., Rigby, P. W., & Tjian, R. (1991). Transcription factor AP-2 is expressed in neural crest cell lineages during mouse embryogenesis. *Genes and Development*, *5*(1), 105–119.

Monk, K. R., Feltri, M. L., & Taveggia, C. (2015). New insights on Schwann cell development. *Glia*, *63*(8), 1376–1393. https://doi.org/10.1002/glia.22852

Nagoshi, N., Shibata, S., Kubota, Y., Nakamura, M., Nagai, Y., Satoh, E., … Okano, H. (2008). Ontogeny and multipotency of neural crest-derived stem cells in mouse bone marrow, dorsal root ganglia, and whisker pad. *Cell Stem Cell*, *2*(4), 392–403. https://doi.org/10.1016/j.stem.2008.03.005

Najm, F. J., Lager, A. M., Zaremba, A., Wyatt, K., Caprariello, A. V., Factor, D. C., … Tesar, P. J. (2013). Transcription factor-mediated reprogramming of fibroblasts to expandable, myelinogenic oligodendrocyte progenitor cells. *Nature Biotechnology*, *31*(5), 426–433. https://doi.org/10.1038/nbt.2561

Nguyen, T. H., Khakhoulina, T., Simmons, A., Morel, P., & Trono, D. (2005). A simple and highly effective method for the stable transduction of uncultured porcine hepatocytes using lentiviral vector. *Cell Transplantation*, *14*(7), 489–496.

Nishimura, E. K., Jordan, S. A., Oshima, H., Yoshida, H., Osawa, M., Moriyama, M., … Nishikawa, S. (2002). Dominant role of the niche in melanocyte stem-cell fate determination. *Nature*, *416*(6883), 854–860. https://doi.org/10.1038/416854a

Peng, J., Wang, Y., Zhang, L., Zhao, B., Zhao, Z., Chen, J., … Lu, S. (2011). Human umbilical cord Wharton's jelly-derived mesenchymal stem cells differentiate into a Schwann-cell phenotype and promote neurite outgrowth in vitro. *Brain Research Bulletin*, *84*(3), 235–243. https://doi.org/10.1016/j.brainresbull.2010.12.013

Rackham, O. J., Firas, J., Fang, H., Oates, M. E., Holmes, M. L., Knaupp, A. S., … Gough, J. (2016). A predictive computational framework for direct reprogramming between human cell types. *Nature Genetics*, *48*(3), 331–335. https://doi.org/10.1038/ng.3487

Reist, N. E., Werle, M. J., & McMahan, U. J. (1992). Agrin released by motor neurons induces the aggregation of acetylcholine receptors at neuromuscular junctions. *Neuron*, *8*(5), 865–868.

Riethmacher, D., Sonnenberg-Riethmacher, E., Brinkmann, V., Yamaai, T., Lewin, G. R., & Birchmeier, C. (1997). Severe neuropathies in mice with targeted mutations in the ErbB3 receptor. *Nature*, *389*(6652), 725–730. https://doi.org/10.1038/39593

Ring, K. L., Tong, L. M., Balestra, M. E., Javier, R., Andrews-Zwilling, Y., Li, G., … Huang, Y. (2012). Direct reprogramming of mouse and human fibroblasts into multipotent neural stem cells with a single factor. *Cell Stem Cell*, *11*(1), 100–109. https://doi.org/10.1016/j.stem.2012.05.018

Salzer, J. L. (2015). Schwann cell myelination. *Cold Spring Harbor Perspectives in Biology*, *7*(8), a020529. https://doi.org/10.1101/cshperspect.a020529

Schreiner, S., Cossais, F., Fischer, K., Scholz, S., Bosl, M. R., Holtmann, B., … Wegner, M. (2007). Hypomorphic Sox10 alleles reveal novel protein functions and unravel developmental differences in glial lineages. *Development*, *134*(18), 3271–3281. https://doi.org/10.1242/dev.003350

Shimizu, S., Kitada, M., Ishikawa, H., Itokazu, Y., Wakao, S., & Dezawa, M. (2007). Peripheral nerve regeneration by the in vitro differentiated-human bone marrow stromal cells with Schwann cell property. *Biochemical and Biophysical Research Communications*, *359*(4), 915–920. https://doi.org/10.1016/j.bbrc.2007.05.212

Stewart, H. J., Brennan, A., Rahman, M., Zoidl, G., Mitchell, P. J., Jessen, K. R., & Mirsky, R. (2001). Developmental regulation and overexpression of the transcription factor AP-2, a potential regulator of the timing of Schwann cell generation. *European Journal of Neuroscience*, *14*(2), 363–372.

Stewart, H. J., Rougon, G., Dong, Z., Dean, C., Jessen, K. R., & Mirsky, R. (1995). TGF-betas upregulate NCAM and L1 expression in cultured Schwann cells, suppress cyclic AMP-induced expression of O4 and galactocerebroside, and are widely expressed in cells of the Schwann cell lineage in vivo. *Glia*, *15*(4), 419–436. https://doi.org/10.1002/glia.440150406

Stolt, C. C., & Wegner, M. (2016). Schwann cells and their transcriptional network: Evolution of key regulators of peripheral myelination. *Brain Research*, *1641*(Pt A), 101–110. https://doi.org/10.1016/j.brainres.2015.09.025

Sudo, K., Kanno, M., Miharada, K., Ogawa, S., Hiroyama, T., Saijo, K., & Nakamura, Y. (2007). Mesenchymal progenitors able to differentiate into osteogenic, chondrogenic, and/or adipogenic cells in vitro are present in most primary fibroblast-like cell populations. *Stem Cells*, *25*(7), 1610–1617. https://doi.org/10.1634/stemcells.2006-0504

Sung, C. C., O'Toole, E. A., Lannutti, B. J., Hunt, J., O'Gorman, M., Woodley, D. T., & Paller, A. S. (1998). Integrin alpha 5 beta 1 expression is required for inhibition of keratinocyte migration by ganglioside GT1b. *Experimental Cell Research*, *239*(2), 311–319. https://doi.org/10.1006/excr.1997.3897

Svaren, J., & Meijer, D. (2008). The molecular machinery of myelin gene transcription in Schwann cells. *Glia*, *56*(14), 1541–1551. https://doi.org/10.1002/glia.20767

Thoma, E. C., Merkl, C., Heckel, T., Haab, R., Knoflach, F., Nowaczyk, C., … Iacone, R. (2014). Chemical conversion of human fibroblasts into

functional Schwann cells. *Stem Cell Reports*, *3*(4), 539–547. https://doi.org/10.1016/j.stemcr.2014.07.014

Tohill, M., Mantovani, C., Wiberg, M., & Terenghi, G. (2004). Rat bone marrow mesenchymal stem cells express glial markers and stimulate nerve regeneration. *Neuroscience Letters*, *362*(3), 200–203. https://doi.org/10.1016/j.neulet.2004.03.077

Topilko, P., Schneider-Maunoury, S., Levi, G., Baron-Van Evercooren, A., Chennoufi, A. B., Seitanidou, T., … Charnay, P. (1994). Krox-20 controls myelination in the peripheral nervous system. *Nature*, *371*(6500), 796–799. https://doi.org/10.1038/371796a0

Varejao, A. S., Meek, M. F., Ferreira, A. J., Patricio, J. A., & Cabrita, A. M. (2001). Functional evaluation of peripheral nerve regeneration in the rat: Walking track analysis. *Journal of Neuroscience Methods*, *108*(1), 1–9.

Vierbuchen, T., Ostermeier, A., Pang, Z. P., Kokubu, Y., Sudhof, T. C., & Wernig, M. (2010). Direct conversion of fibroblasts to functional neurons by defined factors. *Nature*, *463*(7284), 1035–1041. https://doi.org/10.1038/nature08797

Villanueva, S., Glavic, A., Ruiz, P., & Mayor, R. (2002). Posteriorization by FGF, Wnt, and retinoic acid is required for neural crest induction. *Developmental Biology*, *241*(2), 289–301. https://doi.org/10.1006/dbio.2001.0485

Wakao, S., Hayashi, T., Kitada, M., Kohama, M., Matsue, D., Teramoto, N., … Dezawa, M. (2010). Long-term observation of auto-cell transplantation in non-human primate reveals safety and efficiency of bone marrow stromal cell-derived Schwann cells in peripheral nerve regeneration. *Experimental Neurology*, *223*(2), 537–547. https://doi.org/10.1016/j.expneurol.2010.01.022

Wakao, S., Kitada, M., Kuroda, Y., Shigemoto, T., Matsuse, D., Akashi, H., … Dezawa, M. (2011). Multilineage-differentiating stress-enduring (muse) cells are a primary source of induced pluripotent stem cells in human fibroblasts. *Proceedings of the National Academy of Sciences of the United States of America*, *108*(24), 9875–9880. https://doi.org/10.1073/pnas.1100816108

Wang, X., Luo, E., Li, Y., & Hu, J. (2011). Schwann-like mesenchymal stem cells within vein graft facilitate facial nerve regeneration and remyelination. *Brain Research*, *1383*, 71–80. https://doi.org/10.1016/j.brainres.2011.01.098

Wegner, M. (2000). Transcriptional control in myelinating glia: The basic recipe. *Glia*, *29*(2), 118–123.

Weider, M., & Wegner, M. (2017). SoxE factors: Transcriptional regulators of neural differentiation and nervous system development. *Seminars in Cell & Developmental Biology*, *63*, 35–42. https://doi.org/10.1016/j.semcdb.2016.08.013

Woodhoo, A., & Sommer, L. (2008). Development of the Schwann cell lineage: From the neural crest to the myelinated nerve. *Glia*, *56*(14), 1481–1490. https://doi.org/10.1002/glia.20723

Xu, Y., Liu, L., Li, Y., Zhou, C., Xiong, F., Liu, Z., … Zhang, C. (2008). Myelin-forming ability of Schwann cell-like cells induced from rat adipose-derived stem cells in vitro. *Brain Research*, *1239*, 49–55. https://doi.org/10.1016/j.brainres.2008.08.088

Zhu, H., Yang, A., Du, J., Li, D., Liu, M., Ding, F., … Liu, Y. (2014). Basic fibroblast growth factor is a key factor that induces bone marrow mesenchymal stem cells towards cells with Schwann cell phenotype. *Neuroscience Letters*, *559*, 82–87. https://doi.org/10.1016/j.neulet.2013.11.044

Zorick, T. S., Syroid, D. E., Arroyo, E., Scherer, S. S., & Lemke, G. (1996). The transcription factors SCIP and Krox-20 mark distinct stages and cell fates in Schwann cell differentiation. *Molecular and Cellular Neurosciences*, *8*(2–3), 129–145. https://doi.org/10.1006/mcne.1996.0052

Zujovic, V., Doucerain, C., Hidalgo, A., Bachelin, C., Lachapelle, F., Weissert, R., … Baron-Van Evercooren, A. (2012). Exogenous schwann cells migrate, remyelinate and promote clinical recovery in experimental auto-immune encephalomyelitis. *PLoS One*, *7*(9), e42667. https://doi.org/10.1371/journal.pone.0042667

SUPPORTING INFORMATION

Additional supporting information may be found online in the Supporting Information section at the end of the article.

How to cite this article: Kitada M, Murakami T, Wakao S, Li G, Dezawa M. Direct conversion of adult human skin fibroblasts into functional Schwann cells that achieve robust recovery of the severed peripheral nerve in rats. *Glia*. 2018;1–17. https://doi.org/10.1002/glia.23582